

Supporting Information

Mg(II) Heterodinuclear Catalysts Delivering Carbon Dioxide Derived Multi-Block Polymers

Gloria Rosetto,^a Arron C. Deacy^a and Charlotte K. Williams*^a

Chemistry Research Lab, University of Oxford, Mansfield Road, Oxford, UK, OX1 3TA

Contents

Experimental Section.....	4
Materials.....	4
Methods	4
General procedure for reactions under CO ₂	4
General procedure for CO ₂ /N ₂ switch polymerization reactions.....	4
Mass flow Measurements	4
Polymer purification	5
Supporting Schemes, Figures and Data	6
Figure S1: Illustrations of the key reactions occurring during initiation, propagation, and chain transfer for ROCOP of TCA, CHO, and CO ₂ in the presence of 10 equivalents of cyclohexene diol with catalyst 4	6
Figure S2: ¹ H NMR (CDCl ₃ , 400 MHz) spectrum of TCA.	7
Figure S3: ¹ H NMR (CDCl ₃ , 400 MHz) spectrum of PCHC homopolymer.	7
Figure S4: ¹ H NMR (CDCl ₃ , 400 MHz) spectrum of poly(TCA- <i>alt</i> -CHO) homopolymer.....	8
Figure S5: ¹ H NMR (CDCl ₃ , 400 MHz) spectrum of an aliquot taken for the polymerization of TCA/CHO/CO ₂ with catalyst 1 (Table 1, entry 1).	8
Figure S6: Conversion vs time plot using data from <i>in-situ</i> ATR-IR spectroscopy for the polymerization of TCA/CHO/CO ₂ with catalyst 1	9
Figure S7: ¹ H NMR spectrum (CDCl ₃ , 400 MHz) of an aliquot taken for the polymerization of TCA/CHO/CO ₂ with catalyst 2 (Table 1, entry 2).	10
Figure S8: Conversion vs time plot using data from ATR-IR spectroscopy for the polymerization of TCA/CHO/CO ₂ with catalyst 2	10
Figure S9: ¹ H NMR spectra (CDCl ₃ , 400 MHz) of aliquots taken for the polymerization of TCA/CHO/CO ₂ with catalyst 3 (Table 1, entry 3). Bottom spectrum: aliquot taken at 45 min. Top spectrum: aliquot taken at 1h30, showing >99 % conversion of TCA.	11
Figure S10: ¹ H NMR spectra (CDCl ₃ , 400 MHz) of purified polymer in Table 1, entry 3.	11
Figure S11: ¹ H DOSY NMR (CDCl ₃ , 500 MHz) spectrum of the purified random copolymer obtained from the polymerization of TCA/CHO/CO ₂ with catalyst 3	12
Figure S12: Selected regions of the ¹³ C{ ¹ H} NMR (125.8 MHz, CDCl ₃) spectra of poly(PE- <i>b</i> -PCHC) (top) and poly(PE- <i>r</i> -PCHC) (bottom). New signals can be observed at 154 ppm for the random copolymer.	12
Figure S13: ¹ H NMR spectrum (CDCl ₃ , 400 MHz) of an aliquot taken for the polymerization of TCA/CHO/CO ₂ with catalyst 4 (Table 1, entry 4).	13
Figure S14: Conversion vs time plot using data from ATR-IR spectroscopy for the polymerization of TCA/CHO/CO ₂ with catalyst 4	13

Figure S15: ¹ H NMR spectrum (CDCl ₃ , 400 MHz) of an aliquot taken for the polymerization of PA/CHO/CO ₂ with catalyst 1 (Table 1, entry 5).	14
Figure S16: Conversion vs time plot using data from ATR-IR spectroscopy for the polymerization of PA/CHO/CO ₂ with catalyst 1	14
Figure S17: ¹ H NMR spectrum (CDCl ₃ , 400 MHz) of an aliquot taken for the polymerization of PA/CHO/CO ₂ with catalyst 3 (Table 1, entry 7).	15
Figure S18: ¹ H NMR spectrum (CDCl ₃ , 400 MHz) of aliquots taken for the polymerization of PA/CHO/CO ₂ with catalyst 4 (Table 1, entry 8). Bottom: aliquot after 24 min. Top: aliquot after 1 hour	15
Figure S19: ¹ H NMR spectrum (CDCl ₃ , 400 MHz) of an aliquot taken for the polymerization of PA/CHO/CO ₂ with catalyst 2 (Table 1, entry 6).	16
Figure S20: Conversion vs time plot using data from ATR-IR spectroscopy for the polymerization of PA/CHO/CO ₂ with catalyst 2	17
Figure S21: Mass flow of CO ₂ in mLn/min for the polymerization of PA/CHO/CO ₂ with catalyst 4 (Table 1, entry 8).	17
Figure S22: Selected regions of the ¹³ C{ ¹ H} NMR spectra (125.8 MHz, CDCl ₃) of poly(PE'- <i>b</i> -PCHC) (top) and poly(PE'- <i>r</i> -PCHC) (bottom). A sharper peak for the polycarbonate junction unit can be observed at 154 ppm for the random copolymer.	18
Figure S23: ¹ H DOSY NMR spectrum (CDCl ₃ , 500 MHz) of the purified random copolymer obtained from the polymerization of PA/CHO/CO ₂ with catalyst 4	18
Figure S24: Conversion vs time plot using data from ATR-IR spectroscopy for the polymerization of PA/CHO/CO ₂ at 20 bar of CO ₂ with catalyst 4	19
Figure S25: ¹ H NMR spectra (CDCl ₃ , 400 MHz) of aliquots taken during the polymerization of PA/CHO/CO ₂ (20 bar) with catalyst 4 (Table 1, entry 9). Bottom spectrum: after 35 min under 20 bar of CO ₂ . Top spectrum: after 20 min under air.	19
Figure S26: Example ¹ H NMR spectrum (CDCl ₃ , 400 MHz) showing resonances and integrals for a typical TCA/CHO/CO ₂ ROCOP.	20
Figure S27: Example ¹ H NMR spectrum (CDCl ₃ , 400 MHz) showing resonances and integrals for a typical PA/CHO/CO ₂ ROCOP.	20
Figure S28: GPC plot of M _n for catalyst 1 TCA/CHO at 1 bar CO ₂ (Table 1, entry 1)	21
Figure S29: GPC plot of M _n for catalyst 2 TCA/CHO at 1 bar CO ₂ (Table 1, entry 2)	21
Figure S30: GPC plot of M _n for catalyst 3 TCA/CHO at 1 bar CO ₂ (Table 1, entry 3)	21
Figure S31: GPC plot of M _n for catalyst 4 TCA/CHO at 1 bar CO ₂ (Table 1, entry 4)	21
Figure S32: GPC plot of M _n for catalyst 1 PA/CHO at 1 bar CO ₂ (Table 1, entry 5)	22
Figure S33: GPC plot of M _n for catalyst 2 PA/CHO at 1 bar CO ₂ (Table 1, entry 6)	22
Figure S34: GPC plot of M _n for catalyst 3 PA/CHO at 1 bar CO ₂ (Table 1, entry 7)	22
Figure S35: GPC plot of M _n for catalyst 4 PA/CHO at 1 bar CO ₂ (Table 1, entry 8)	22
Figure S37: Diagram of the steel triple manifold Schlenk line used to reversibly switch between CO ₂ , N ₂ , and vacuum.	23
Figure S38: Photograph of the steel triple manifold Schlenk line. CO ₂ pressure is regulated and controlled with a Bronkhorst pressure controller, such that when the pressure drops below the set pressure (due to CO ₂ consumption), the system is automatically pressurized. Mass flow measurements can be recorded using the mass flow metre.	23

Figure S39: Example raw data from the mass flow controller, showing the periodic increase in CO ₂ mass flow as CO ₂ is being consumed throughout the reaction.	24
Figure S40: GPC traces illustrating the increase in molecular weight with block formation during the polymerization with one CO ₂ /N ₂ gas switches (Table 2, entry 1).	24
Figure S41: Conversion vs time plot using data from ATR-IR spectroscopy for the polymerization of TCA/CHO/CO ₂ with catalyst 4, which was switched to a N ₂ atmosphere after 1.3 h.	25
Figure S42: Selected regions of ¹ H NMR spectra of reaction aliquots illustrating the changes in resonances during the different stages of the ABA triblock formation (Table 2, entry 1).	26
Figure S43: Frequency of CO ₂ flow extracted from mass flow data for the polymerization in Table 2, entry 1, which was switched to a N ₂ atmosphere after 1 h.	26
Figure S44: ¹ H DOSY NMR spectrum (CDCl ₃ , 500 MHz) of the purified ABA triblock.	27
Figure S45: Conversion vs time plot using data from ATR-IR spectroscopy for the polymerization of TCA/CHO/CO ₂ with catalyst 4, which was switched to a N ₂ atmosphere after 1 h and back to CO ₂ after 2.3 h under N ₂ (Table 2, entry 2).	27
Figure S46: Selected region of ¹ H NMR spectra of reaction aliquots illustrating the changes in resonances during the different stages of the BABAB pentablock formation (Table 2, entry 2).	28
Figure S47: GPC traces illustrating the increase in molecular weight with block formation during the polymerization with two CO ₂ /N ₂ gas switches (Table 2, entry 2).	28
Figure S48: Frequency of CO ₂ flow extracted from mass flow data for the polymerization in Table 2, entry 2, which was switched to a N ₂ atmosphere after 1 h and switched back to CO ₂ after 2.3 h.	29
Figure S49: Selected region of ¹ H NMR spectra of reaction aliquots illustrating the changes in resonances during the different stages of the ABABABA heptablock formation (Table 2, entry 3).	30
Figure S50: DSC trace of the purified ABA polymer (Table 2, entry 1).	30
Figure S51: DSC trace of the purified BABAB polymer (Table 2, entry 2).	31
Figure S52: Selected region of the ¹ H NMR spectra of reaction aliquots illustrating the changes in resonances during the different stages of the CHO/TCA/CO ₂ /DL polymerization.	31
Figure S53: Selected region of the ¹ H NMR spectra of reaction aliquots illustrating the changes in resonances during the different stages of the CHO/TCA/DL polymerization.	32
Figure S54: GPC traces corresponding to two aliquots taken for the polymerization of CHO/TCA/DL.	32
Figure S55: Catalytic cycles accessed during the switchable catalysis using CHO/CO ₂ /TCA/CL.	33
Figure S56: Stack plot showing the ¹ H NMR spectra of aliquots removed during formation of the polymer blocks.	34
Figure S57: ¹ H NMR spectrum (CDCl ₃ , 400 MHz) of the purified multiblock polymer CABAC.	36
Figure S58: ¹ H DOSY spectrum (CDCl ₃ , 500 MHz) of the purified multiblock polymer CABAC.	36
Figure S59: DSC thermogram of the purified multiblock polymer CABAC.	36
References.	36

Experimental Section

Materials

All experiments were carried out under N₂, using standard Schlenk techniques or in a Mbraun glovebox. Toluene was dried through a solvent purification system, degassed by freeze pump thaw techniques, and stored over 3 Å molecular sieves, under nitrogen. Cyclohexene oxide (Acros Organics) was fractionally distilled three times, once over CaH₂, under N₂, at atmospheric pressure and twice from nBuLi, under reduced pressure. Tricyclic anhydride (TCA) was prepared according to a literature procedure,¹ then recrystallized in hexane and sublimed under vacuum at 90 °C prior to use. Purification of phthalic anhydride (Sigma Aldrich) was achieved through stirring in dry toluene, filtering, recrystallizing from hot chloroform, and subsequently subliming under vacuum at 80 °C. ε-Decalactone (Sigma Aldrich) was dried over CaH₂, followed by fractional distillation under partial vacuum (0.1 mbar) at 70 °C. ε-Caprolactone (Sigma Aldrich) was dried over CaH₂, followed by fractional distillation under partial vacuum (1.2 mbar) at 65 °C. 1,2-Cyclohexanediol (Sigma Aldrich) was recrystallized from ethyl acetate and stored under an inert atmosphere. CP Grade (BOC, 99.995 %) CO₂ was used for all copolymerization studies and dried through two VICI purifier columns at point of use. Catalysts 1-4 were prepared according to literature procedures.²⁻⁵ All other reagents were used as received without further purification.

Methods

¹H NMR spectra were obtained using a Bruker AVIII HD nanobay NMR spectrometer, ¹H DOSY NMR spectra were obtained using a Bruker Avance III NMR spectrometer, and ¹³C NMR spectra were obtained using a Bruker Avance NMR spectrometer. GPC analysis was carried out on a Shimadzu LC-20AD instrument, equipped with a Refractive Index (RI) detector and two PSS SDV 5 μm linear M columns. HPLC grade THF was used as the eluent, at 1.0 mL/min, at 30 °C. Samples were passed through 0.2 μm PTFE filters prior to analysis. Monodisperse polystyrene standards were used for calibration. Most experiments were monitored by *in-situ* ATR-IR spectroscopy, using a Mettler-Toledo ReactIR 4000 spectrometer equipped with a silver halide DiComp probe. Thermal properties were measured using a Mettler Toledo DSC3 Star calorimeter, under N₂ flow (80 mL min⁻¹), referenced with a sealed empty crucible and calibrated using indium. Samples were heated and cooled from 30 to 200 °C, at a rate of 20 °C min⁻¹. Glass transition temperatures (*T*_g) were determined from the midpoint of the transition in the second heating curve.

General procedure for reactions under CO₂

The catalyst (8 μmol), anhydride (0.8 mmol), and epoxide (16 mmol) were combined in a 3 neck screw cap Schlenk tube, with a screw-capped sidearm, in the glovebox. The Schlenk tube was cycled three times, between vacuum and 1 bar of CO₂, and the headspace was evacuated and refilled with 1 bar of CO₂ three times before placing the flask in a pre-heated 100 °C oil bath. Aliquots for ¹H NMR and GPC analysis were taken by extracting 0.1 mL of the mixture with a syringe under a positive flow of reaction gas using the screw-cap sidearm.

General procedure for CO₂/N₂ switch polymerization reactions

The catalyst, monomers, and solvent were combined in a 3 neck screw cap Schlenk tube, with a screw-capped sidearm, in the glovebox. The Schlenk tube was cycled three times on a triple manifold glass Schlenk line, between vacuum and CO₂, and the headspace was evacuated and refilled with CO₂ three times before placing the flask in a pre-heated 100 °C oil bath. To switch to a N₂ atmosphere after the allotted time, CO₂ was removed by applying 6 rapid vacuum/N₂ cycles to the reaction flask. The reaction was left under N₂ for the desired time. The same procedure applies when switching back to CO₂. Aliquots were taken by extracting 0.1 mL of the mixture with a syringe, under a positive flow of reaction gas, using the screw-cap sidearm. Entries in Table 2 were run twice, to be monitored by *in situ* ATIR-IR.

Mass flow Measurements

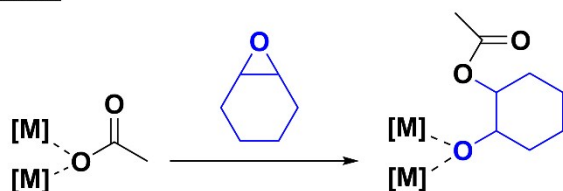
The same procedure as above was repeated on a triple manifold steel Schlenk line, equipped with a pressure controller and mass flow metre (See Figure S37 and 38 for a diagram and image). From the raw mass flow data obtained in millilitre normal per minute (mLn/min) (see example S39), the number of times CO₂ mass flow increased to a maximum was calculated and used qualitatively to show CO₂ uptake.

Polymer purification

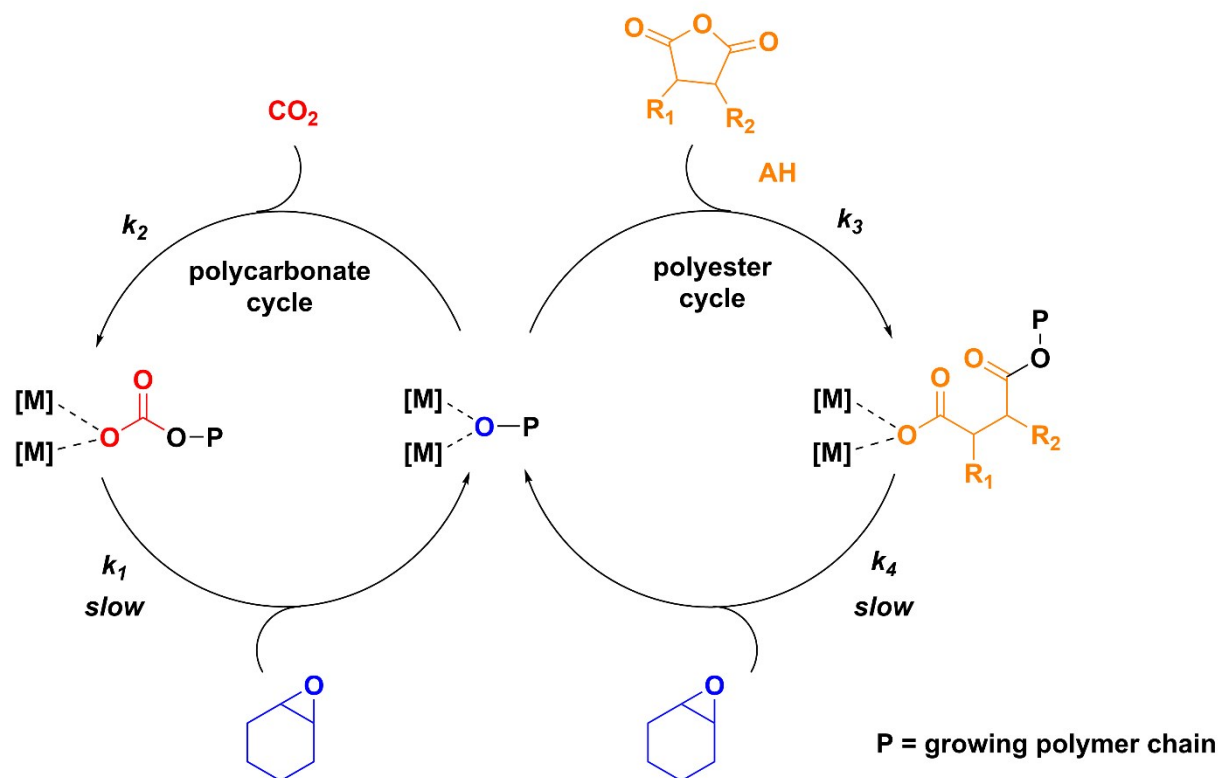
Excess CHO was removed *in vacuo*, and the resulting polymer was purified by precipitation of a DCM solution in acidified methanol. The polymers were dried in a vacuum oven at 60 °C. All the purified polymers were isolated as white or off-white solids.

Supporting Schemes, Figures and Data

Initiation



Propagation



Chain Transfer Equilibria

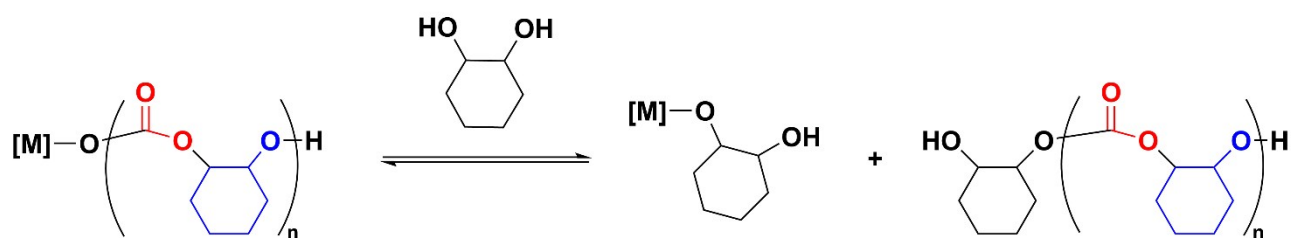


Figure S1: Illustrations of the key reactions occurring during initiation, propagation, and chain transfer for ROCOP of TCA, CHO, and CO_2 in the presence of 10 equivalents of cyclohexene diol with catalyst **4**.

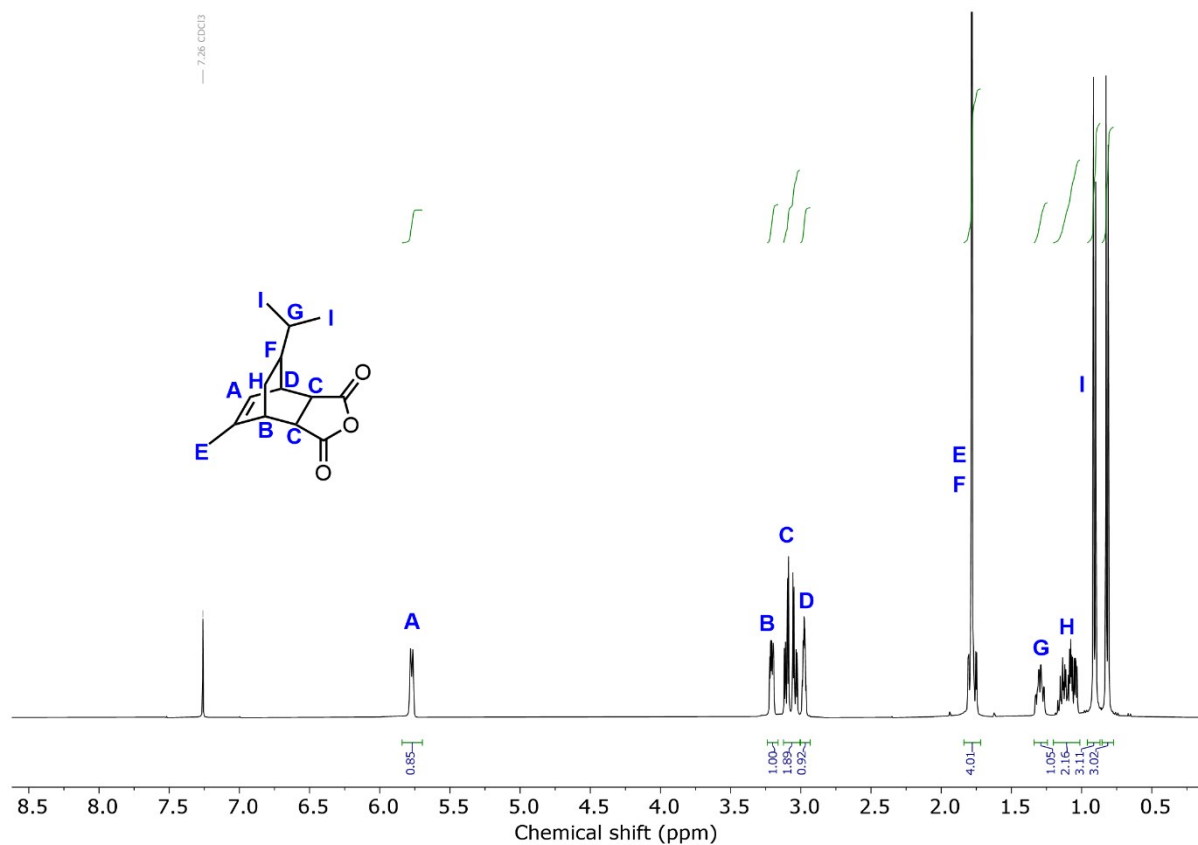


Figure S2: ^1H NMR (CDCl_3 , 400 MHz) spectrum of TCA.

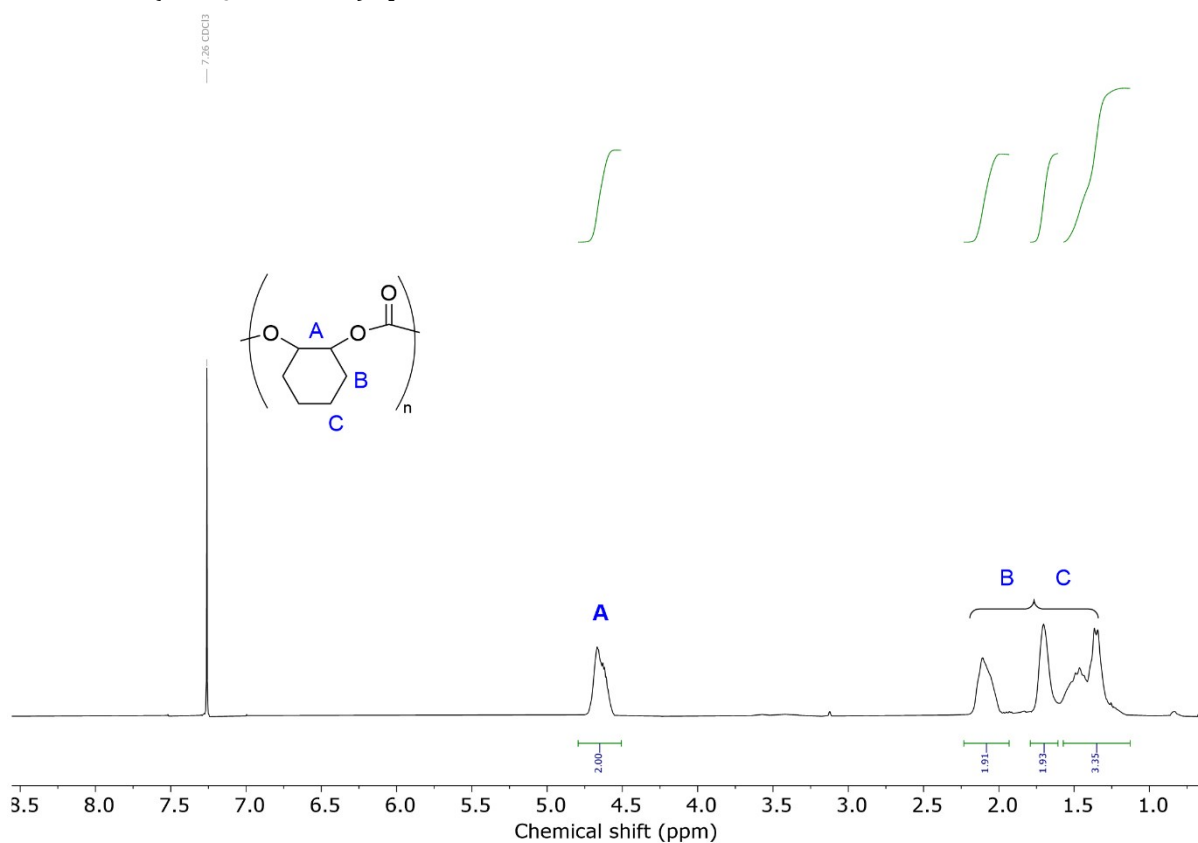


Figure S3: ^1H NMR (CDCl_3 , 400 MHz) spectrum of PCHC homopolymer.

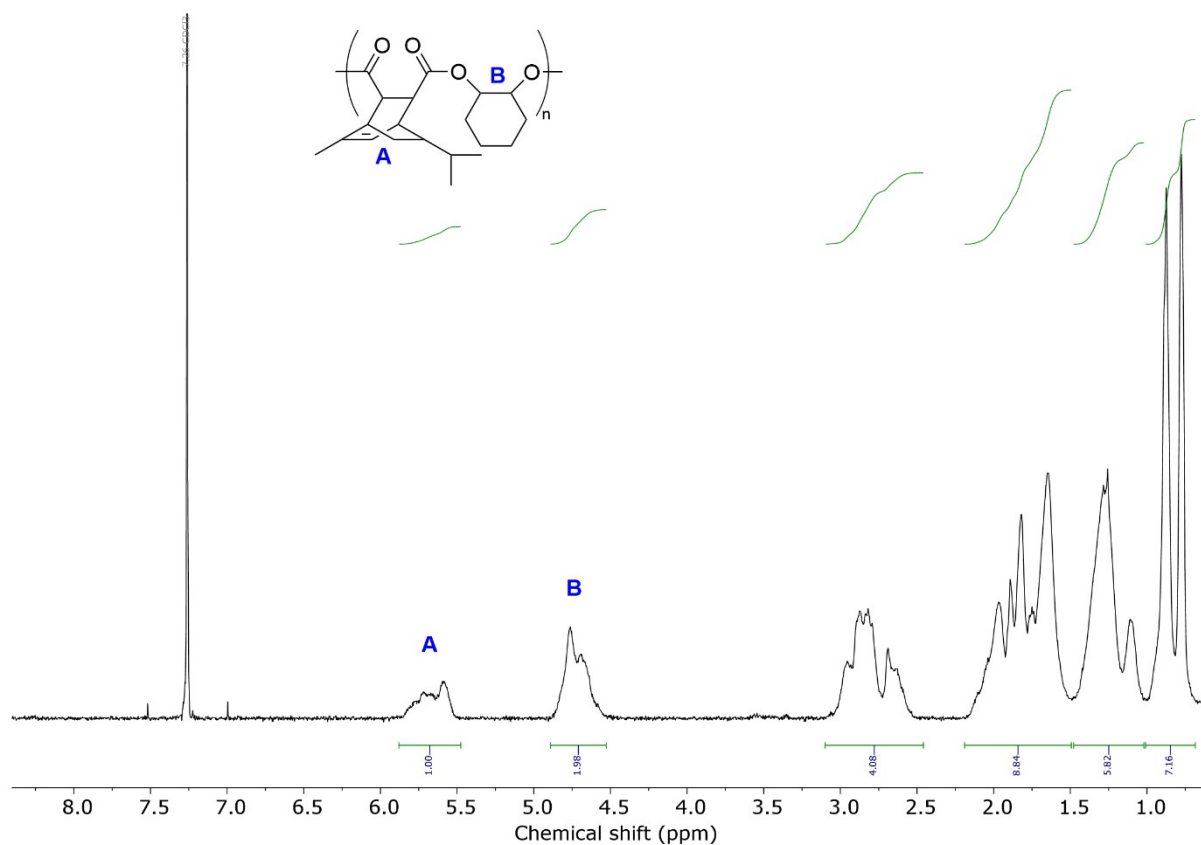


Figure S4: ^1H NMR (CDCl_3 , 400 MHz) spectrum of poly(TCA-*alt*-CHO) homopolymer.

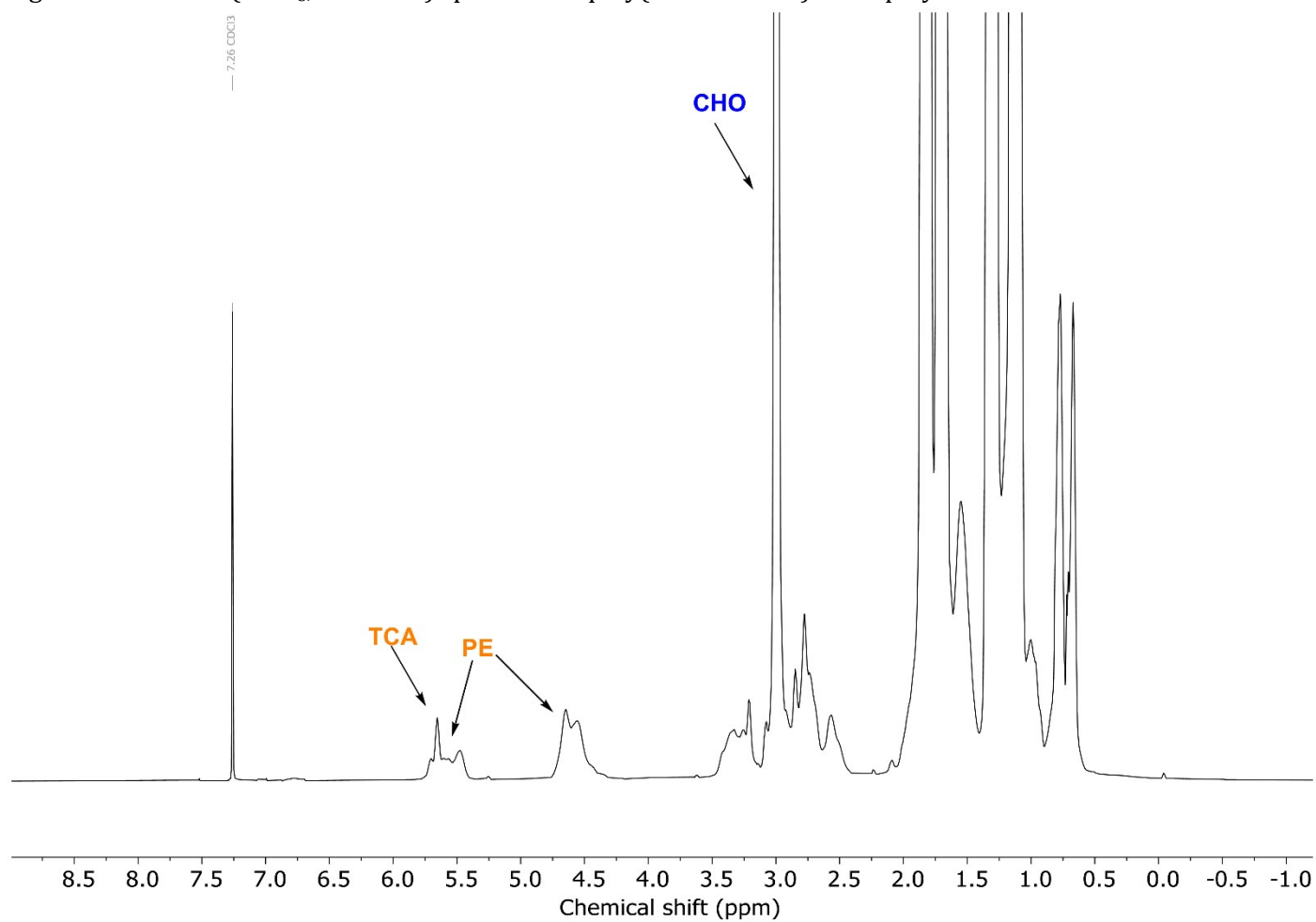


Figure S5: ^1H NMR (CDCl_3 , 400 MHz) spectrum of an aliquot taken for the polymerization of TCA/CHO/ CO_2 with catalyst **1** (Table 1, entry 1).

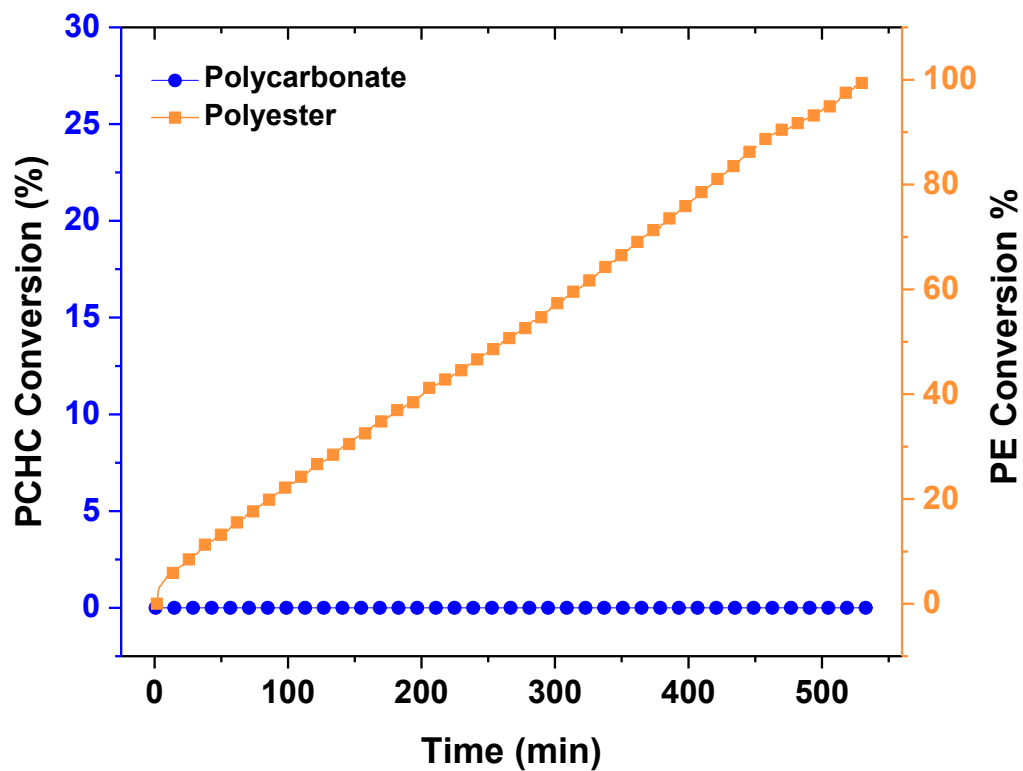


Figure S6: Conversion vs time plot using data from *in-situ* ATR-IR spectroscopy for the polymerization of TCA/CHO/CO₂ with catalyst **1**.

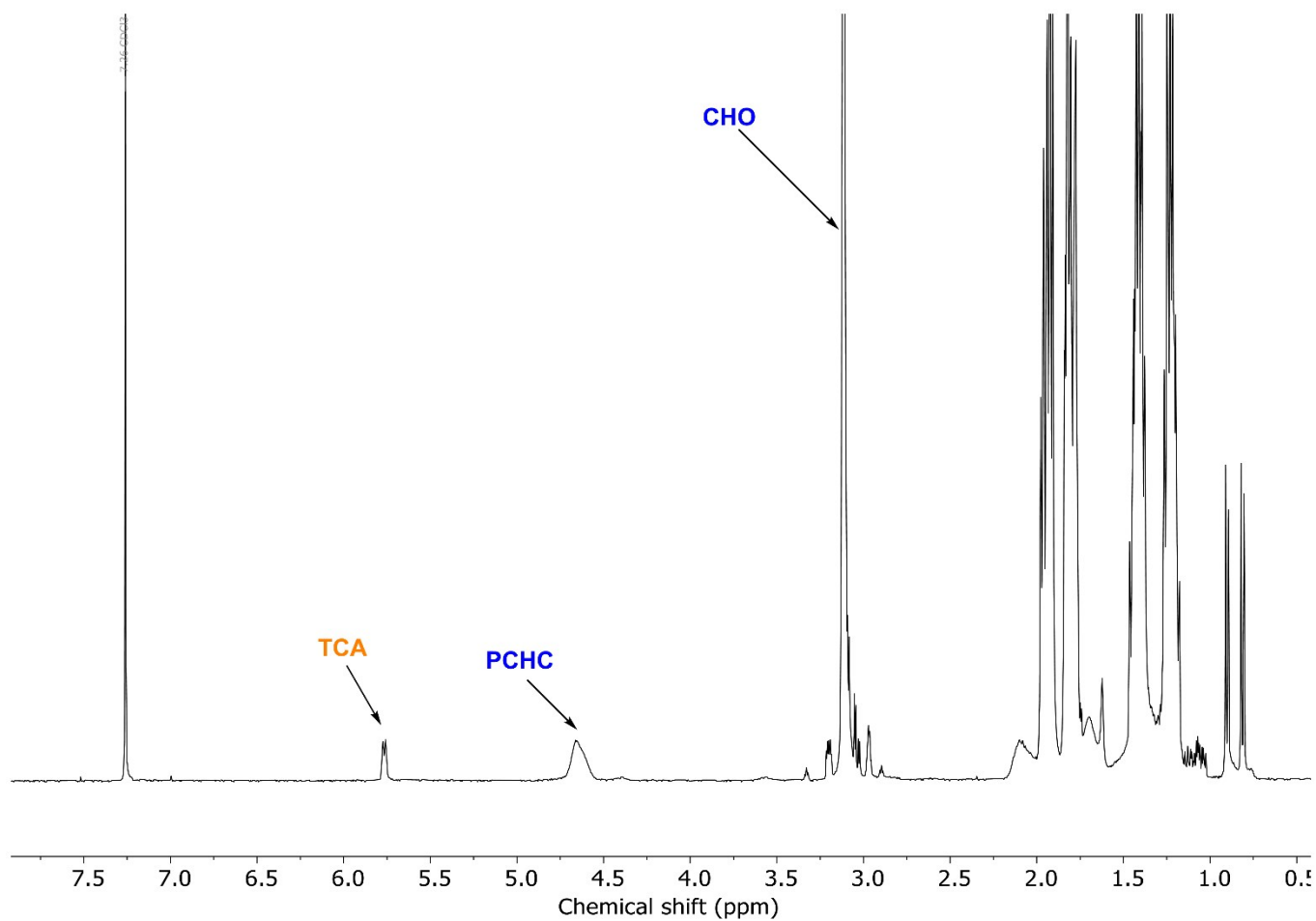


Figure S7: ¹H NMR spectrum (CDCl₃, 400 MHz) of an aliquot taken for the polymerization of TCA/CHO/CO₂ with catalyst **2** (Table 1, entry 2).

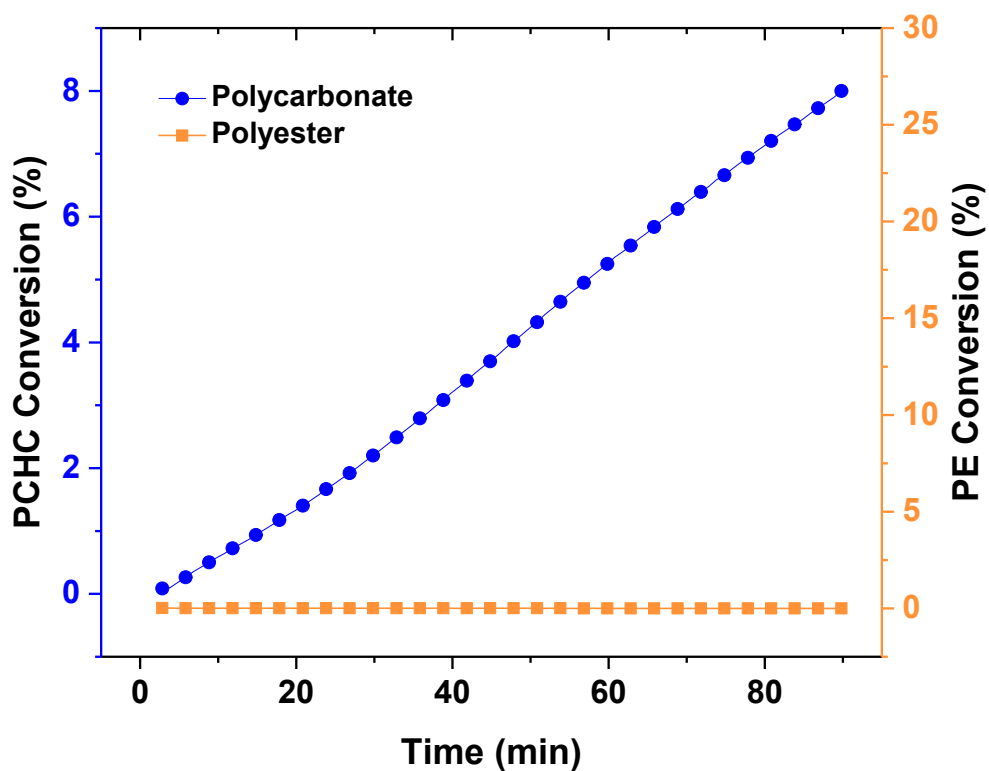


Figure S8: Conversion vs time plot using data from ATR-IR spectroscopy for the polymerization of TCA/CHO/CO₂ with catalyst **2**.

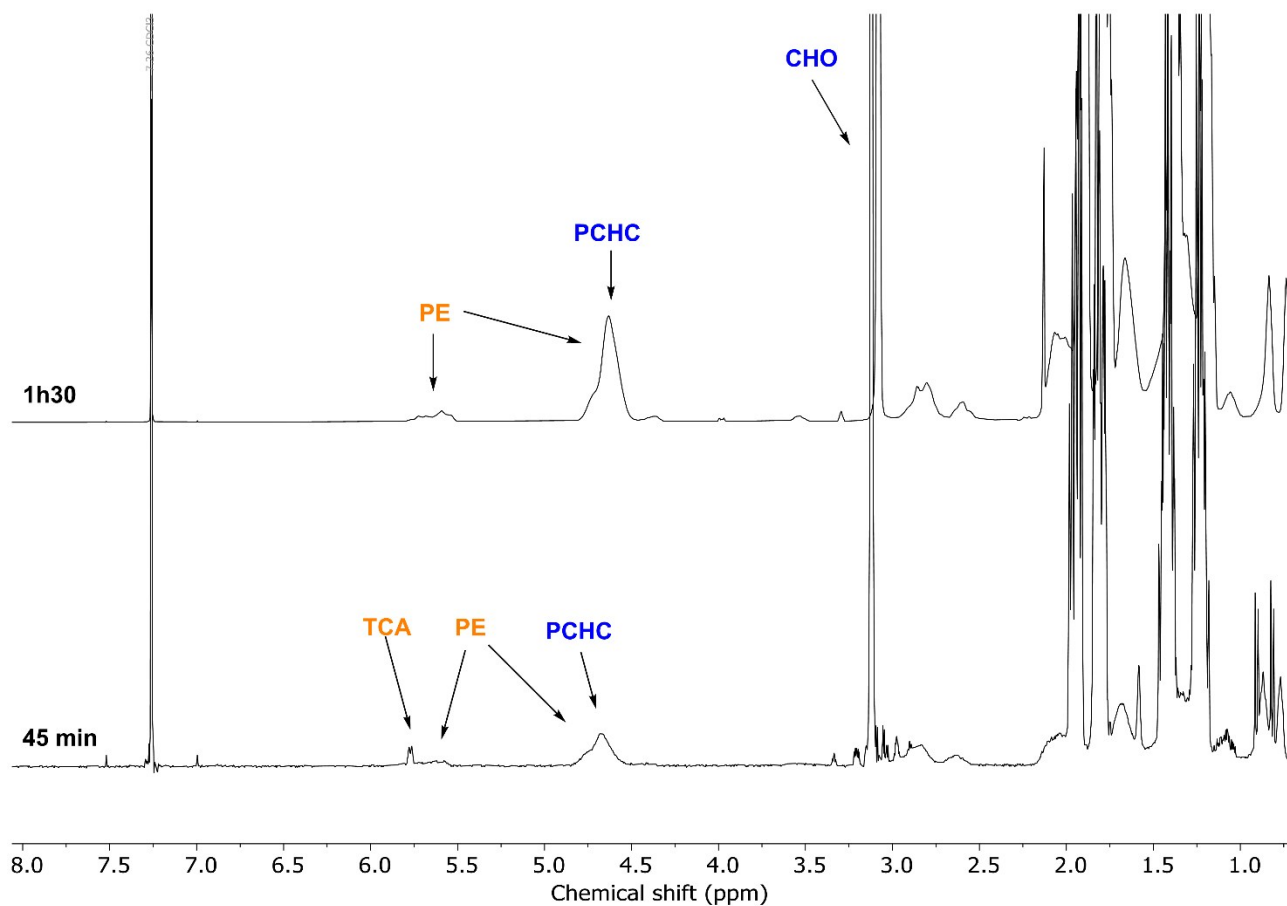


Figure S9: ^1H NMR spectra (CDCl_3 , 400 MHz) of aliquots taken for the polymerization of TCA/CHO/ CO_2 with catalyst **3** (Table 1, entry 3). Bottom spectrum: aliquot taken at 45 min. Top spectrum: aliquot taken at 1h30, showing >99 % conversion of TCA.

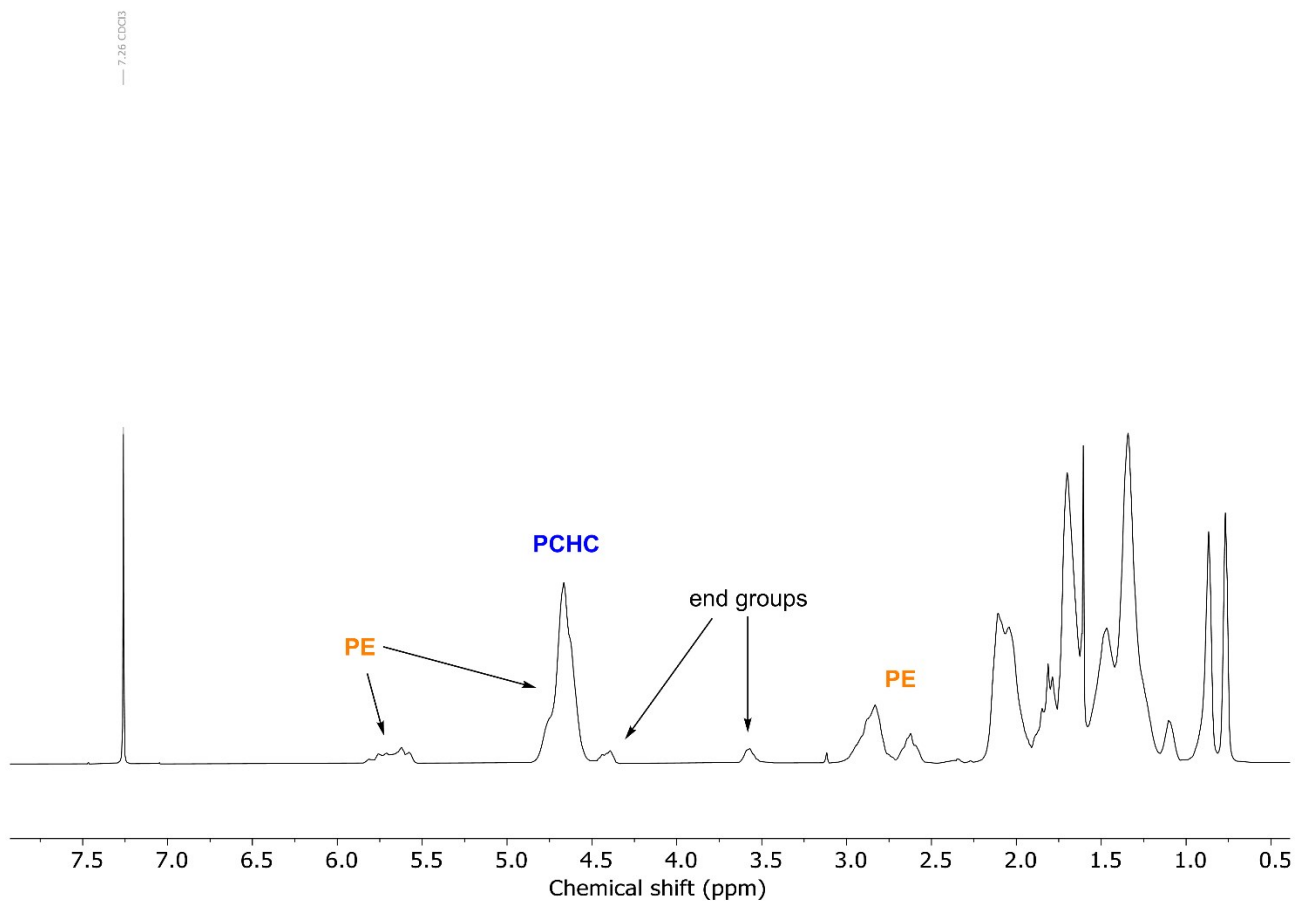


Figure S10: ^1H NMR spectra (CDCl_3 , 400 MHz) of purified polymer in Table 1, entry 3.

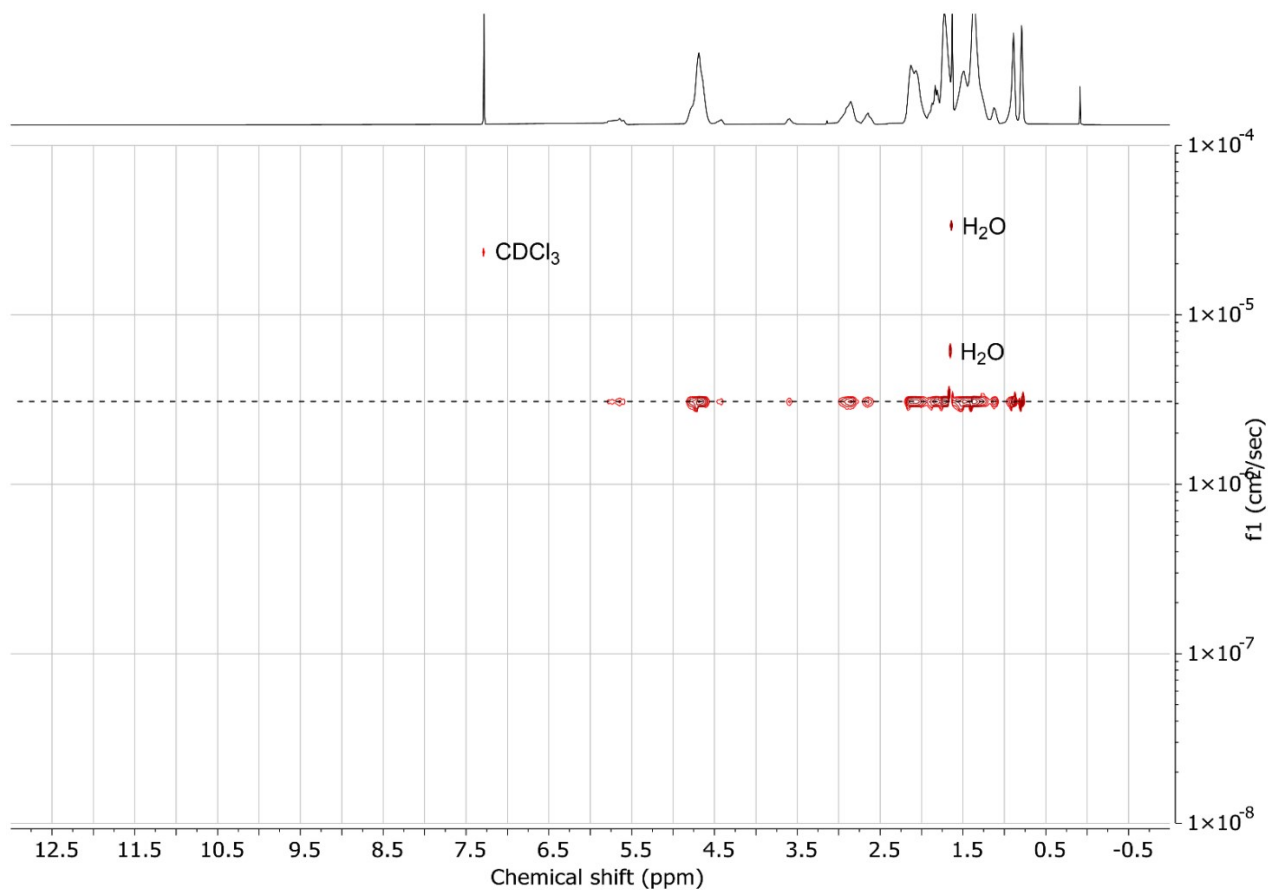
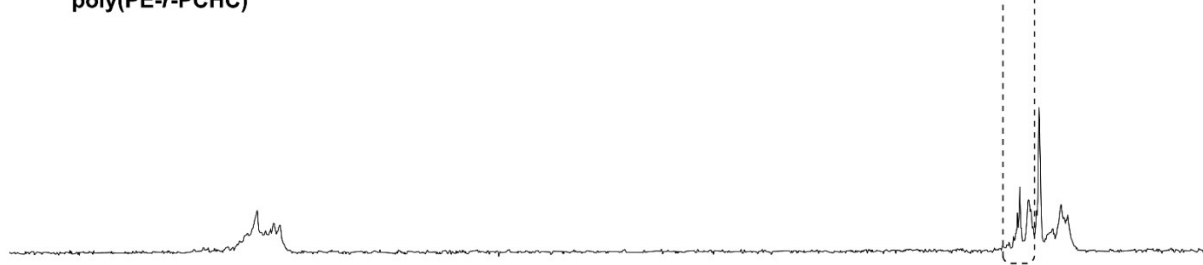


Figure S11: ^1H DOSY NMR (CDCl_3 , 500 MHz) spectrum of the purified random copolymer obtained from the polymerization of TCA/CHO/ CO_2 with catalyst **3**.

poly(PE-*b*-PCHC)



poly(PE-*r*-PCHC)



177 176 175 174 173 172 171 170 169 168 167 166 165 164 163 162 161 160 159 158 157 156 155 154 153 152 151 15
Chemical shift (ppm)

Figure S12: Selected regions of the $^{13}\text{C}\{^1\text{H}\}$ NMR (125.8 MHz, CDCl_3) spectra of poly(PE-*b*-PCHC) (top) and poly(PE-*r*-PCHC) (bottom). New signals can be observed at 154 ppm for the random copolymer.

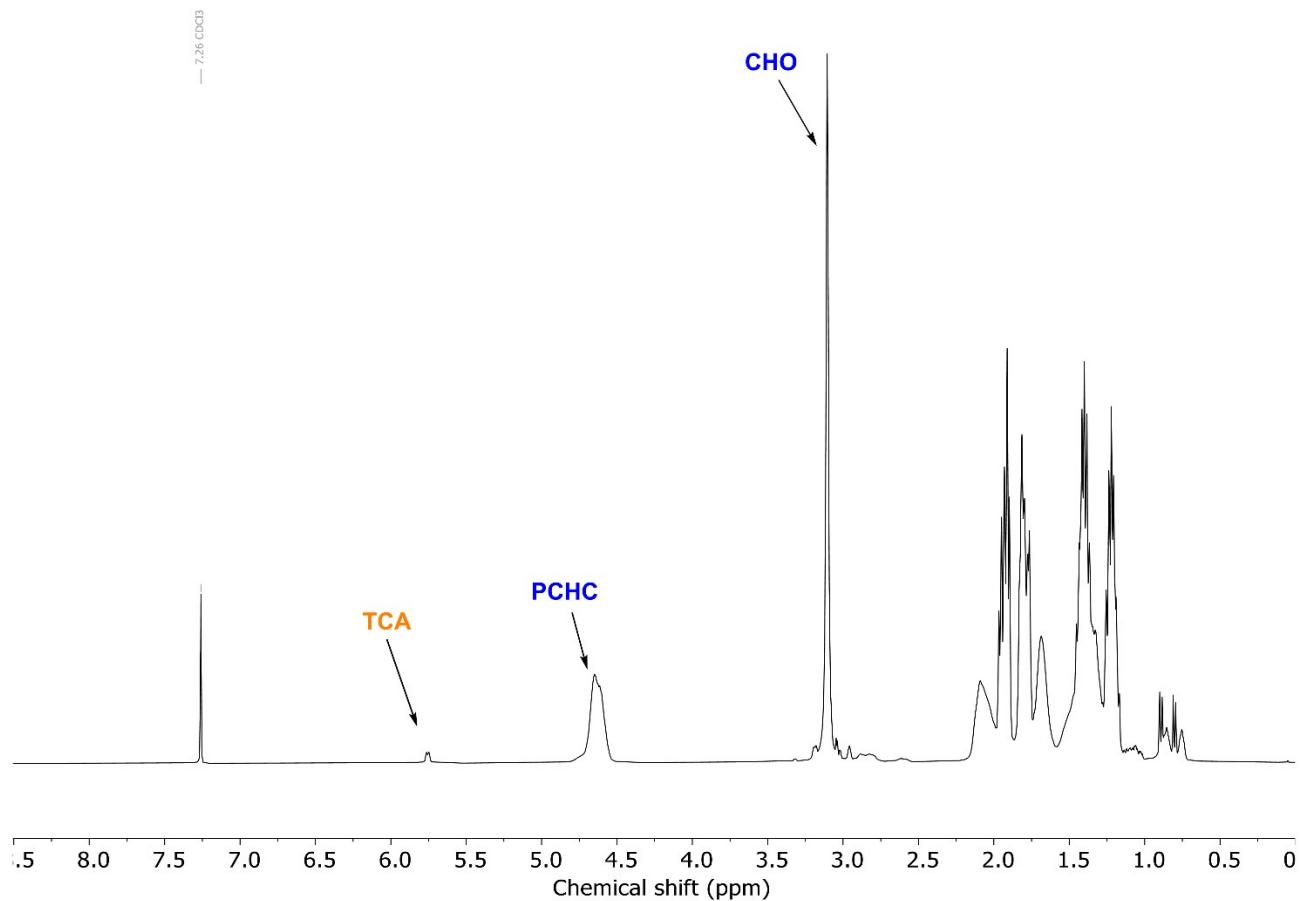


Figure S13: ^1H NMR spectrum (CDCl₃, 400 MHz) of an aliquot taken for the polymerization of TCA/CHO/CO₂ with catalyst **4** (Table 1, entry 4).

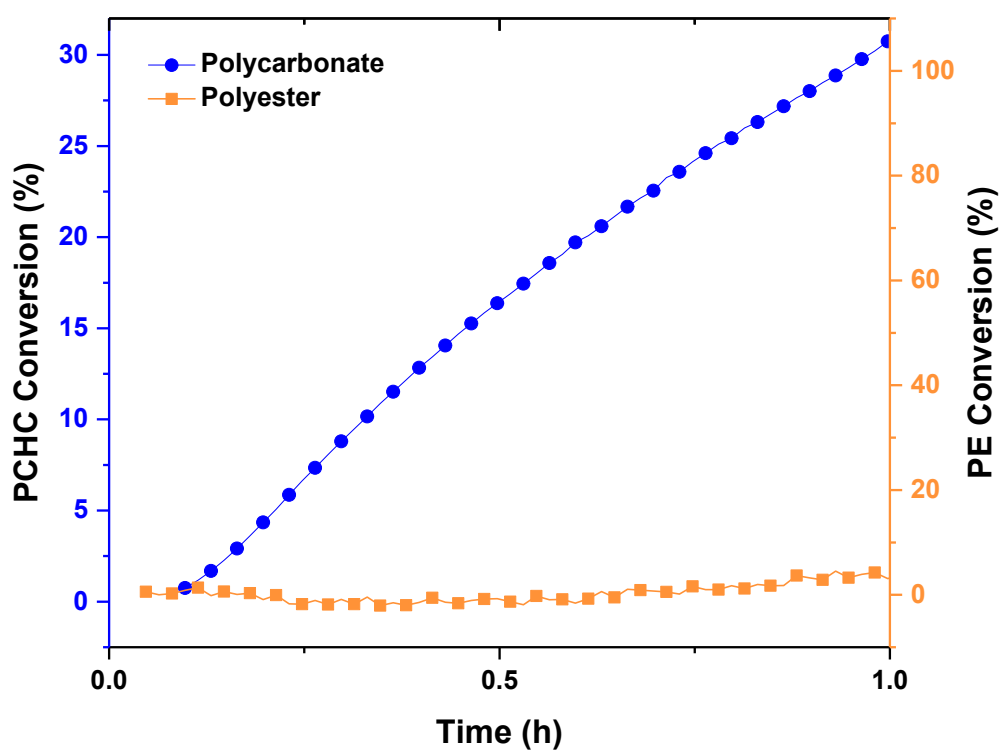


Figure S14: Conversion vs time plot using data from ATR-IR spectroscopy for the polymerization of TCA/CHO/CO₂ with catalyst **4**.

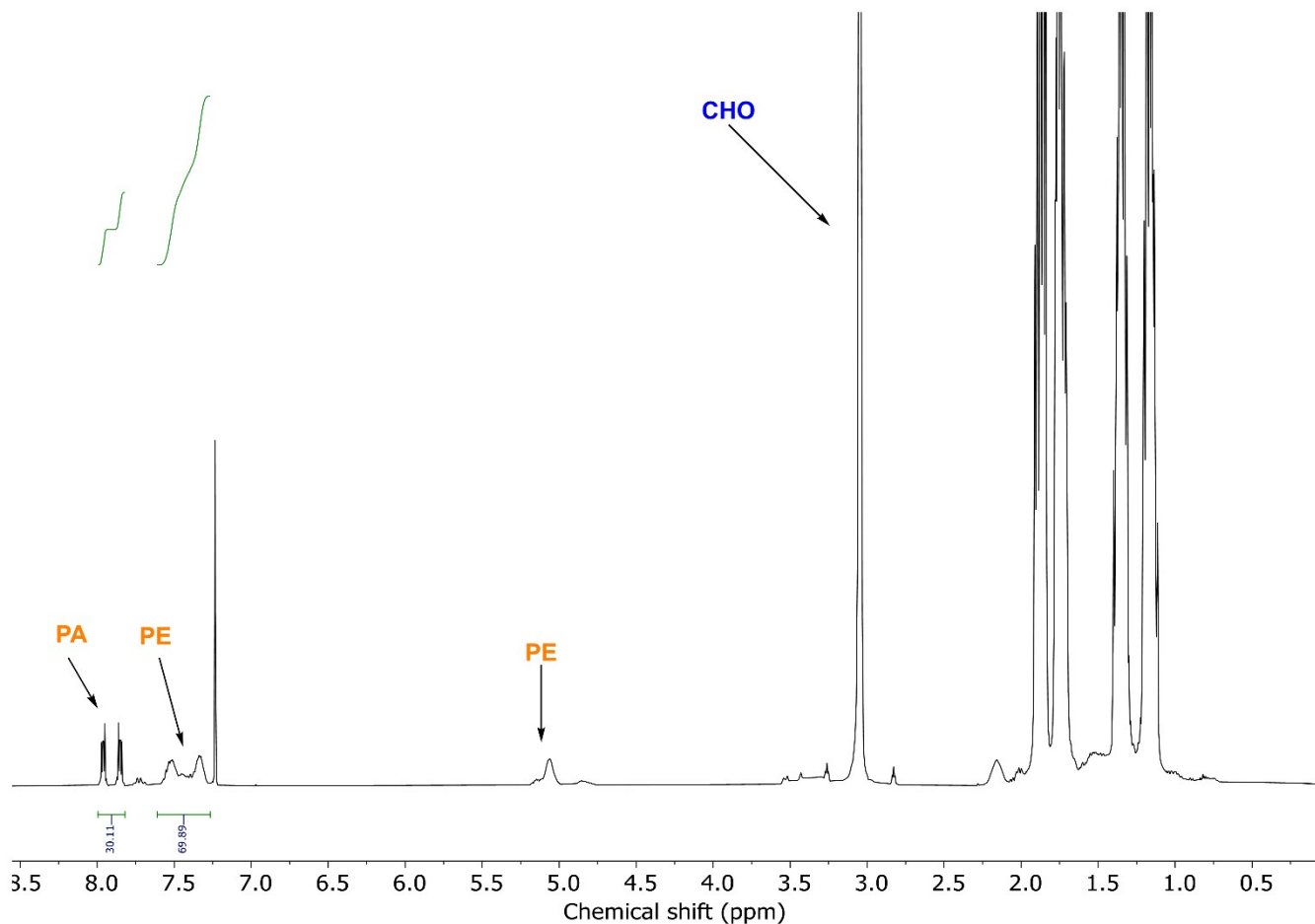


Figure S15: ¹H NMR spectrum (CDCl₃, 400 MHz) of an aliquot taken for the polymerization of PA/CHO/CO₂ with catalyst **1** (Table 1, entry 5).

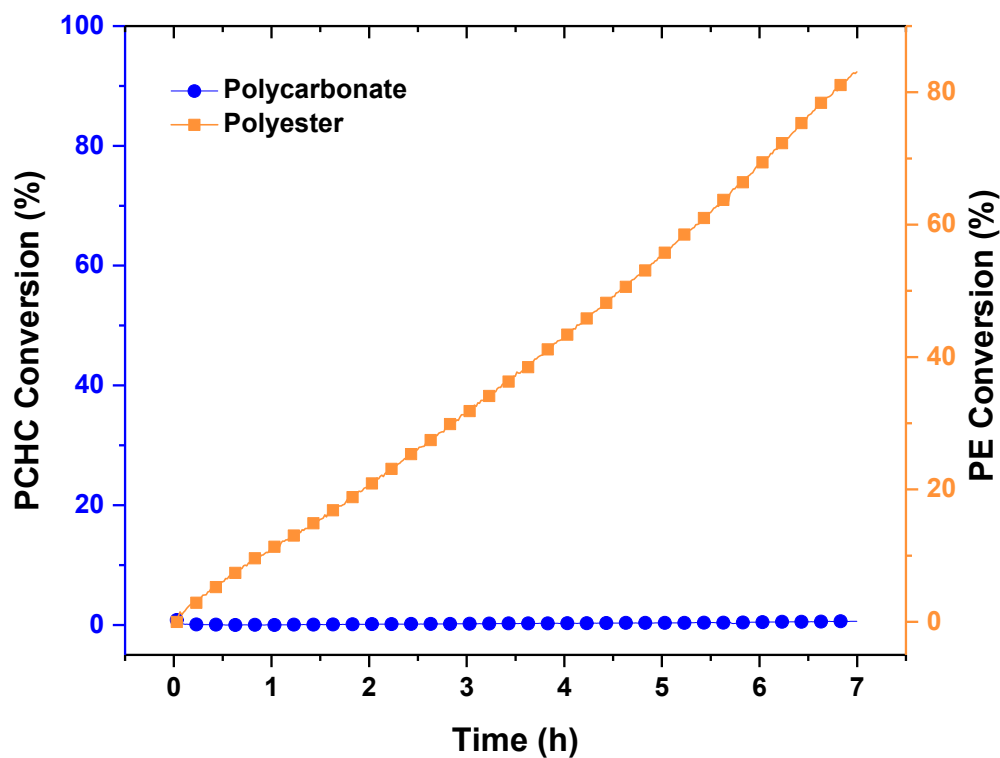


Figure S16: Conversion vs time plot using data from ATR-IR spectroscopy for the polymerization of PA/CHO/CO₂ with catalyst **1**.

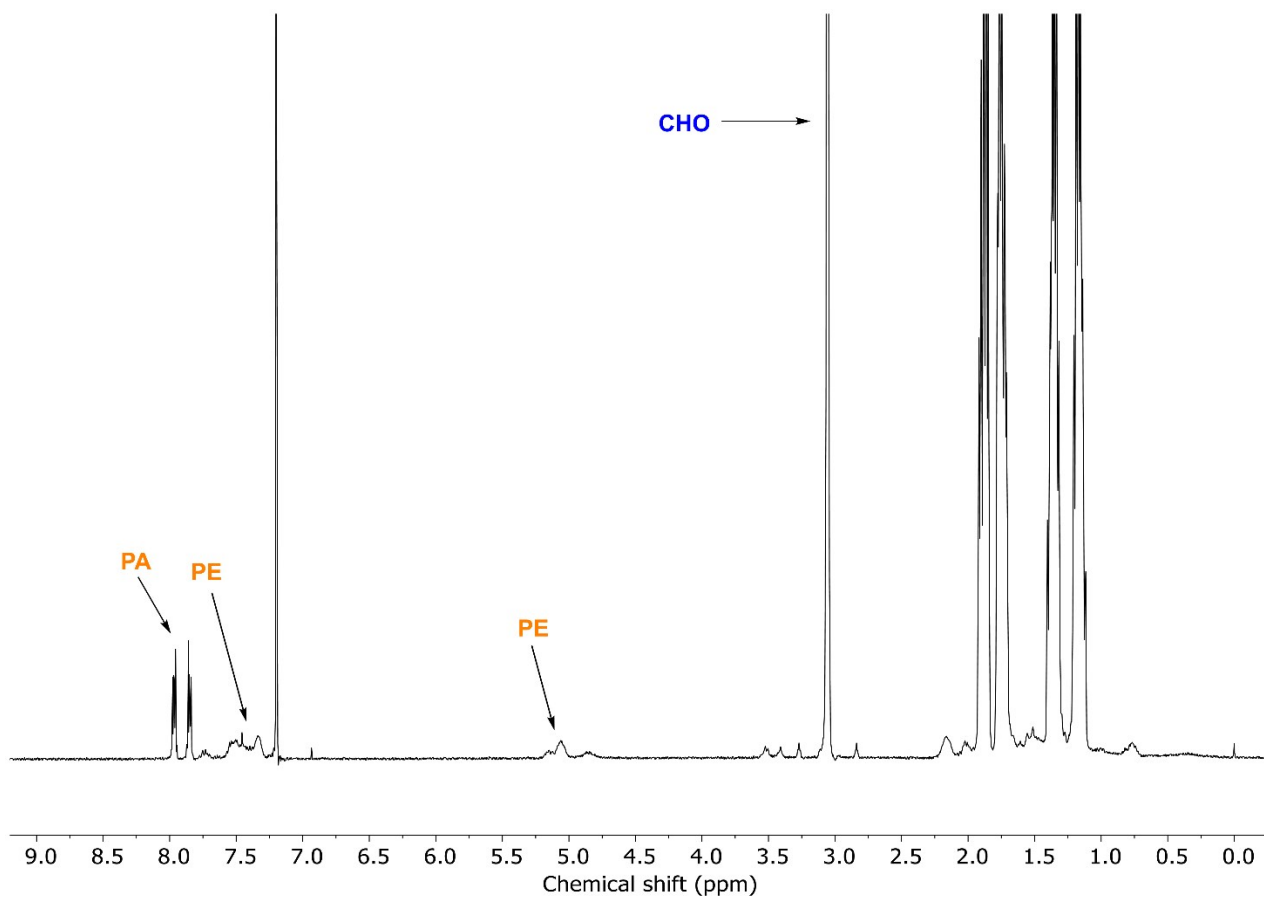


Figure S17: ^1H NMR spectrum (CDCl_3 , 400 MHz) of an aliquot taken for the polymerization of PA/CHO/ CO_2 with catalyst **3** (Table 1, entry 7).

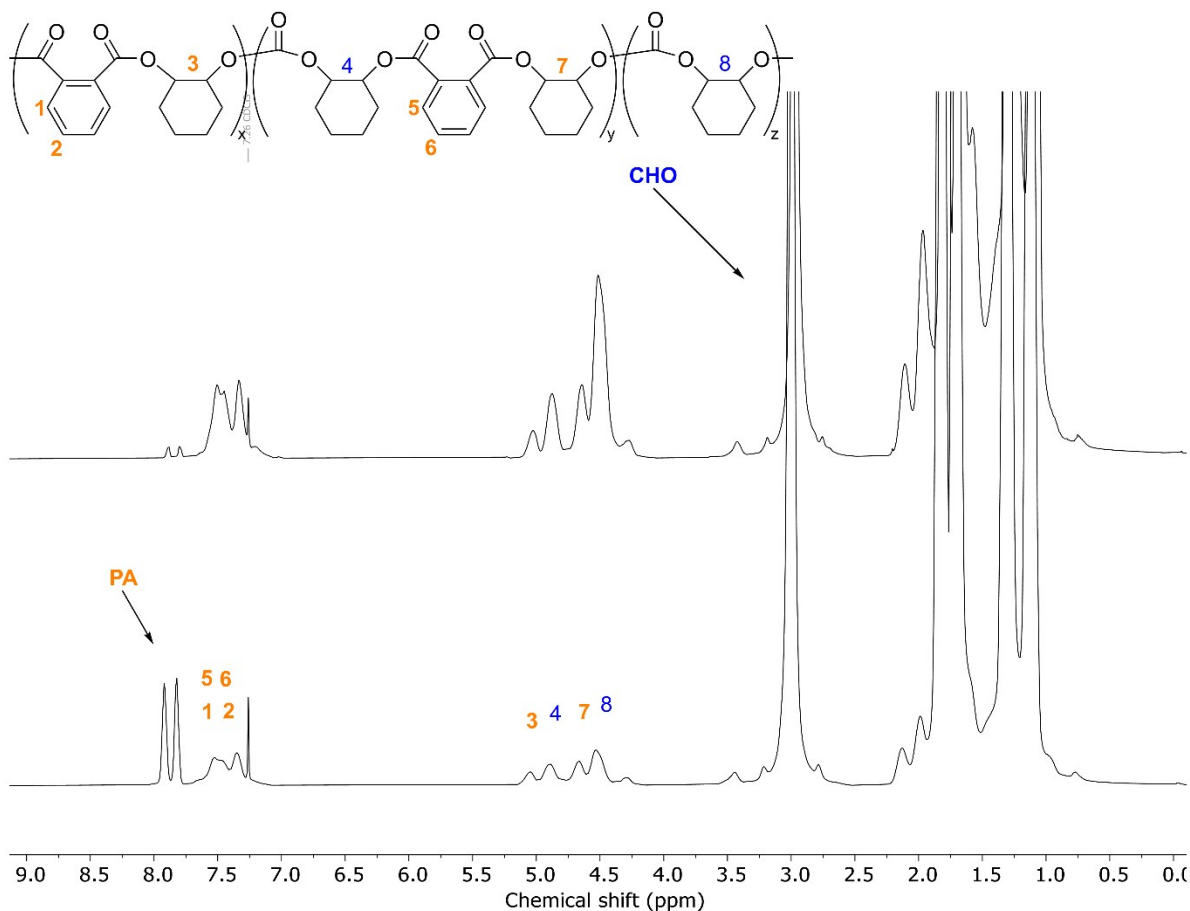


Figure S18: ^1H NMR spectrum (CDCl_3 , 400 MHz) of aliquots taken for the polymerization of PA/CHO/ CO_2 with catalyst **4** (Table 1, entry 8). Bottom: aliquot after 24 min. Top: aliquot after 1 hour

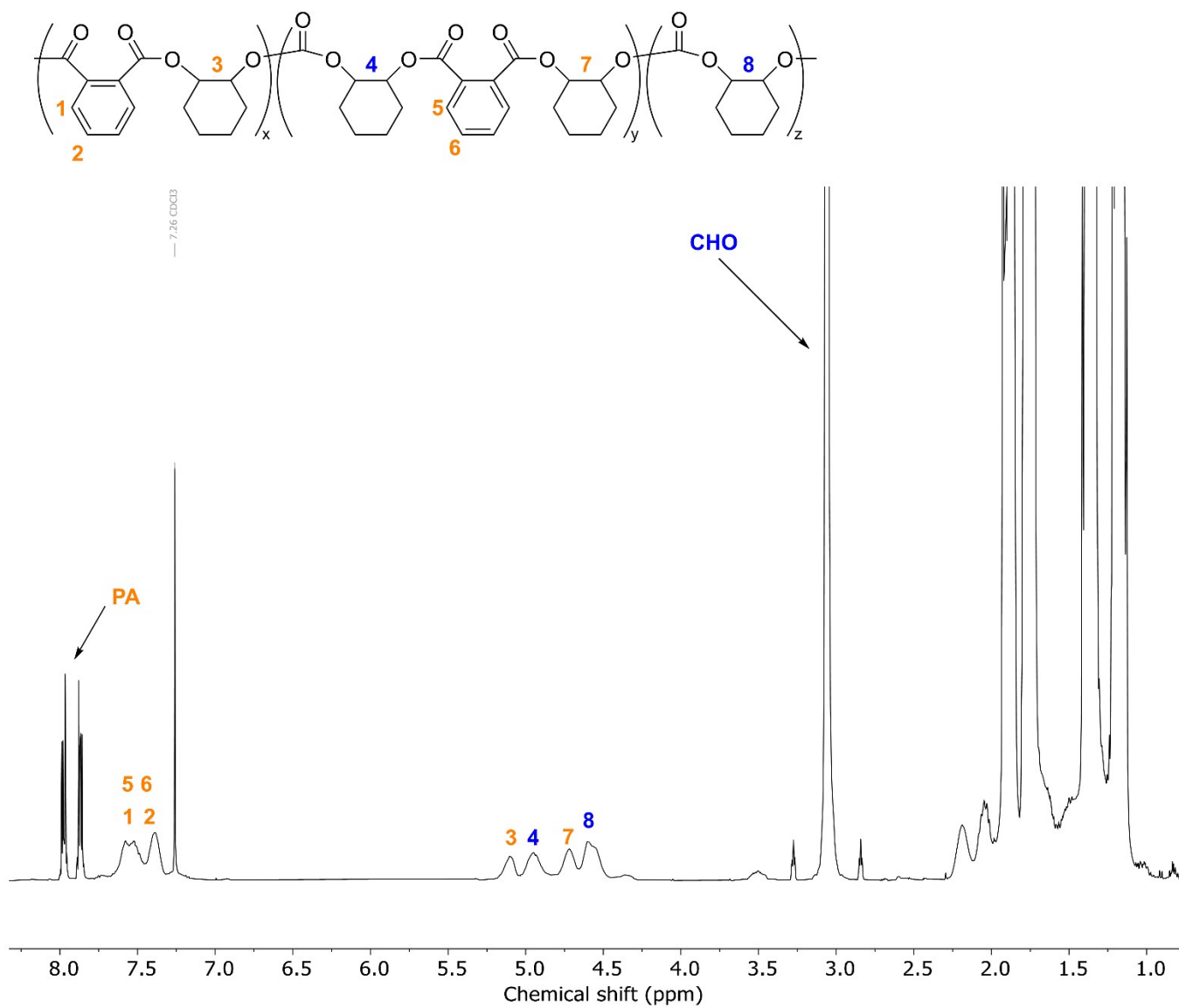


Figure S19: ^1H NMR spectrum (CDCl_3 , 400 MHz) of an aliquot taken for the polymerization of PA/CHO/ CO_2 with catalyst **2** (Table 1, entry 6).

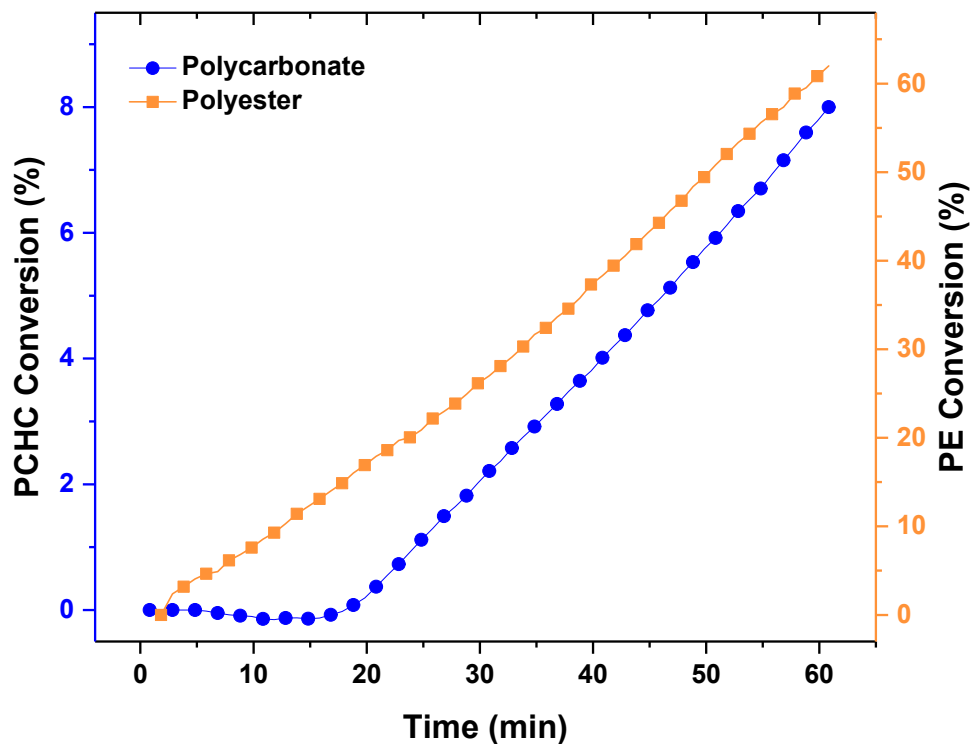


Figure S20: Conversion vs time plot using data from ATR-IR spectroscopy for the polymerization of PA/CHO/CO₂ with catalyst 2.

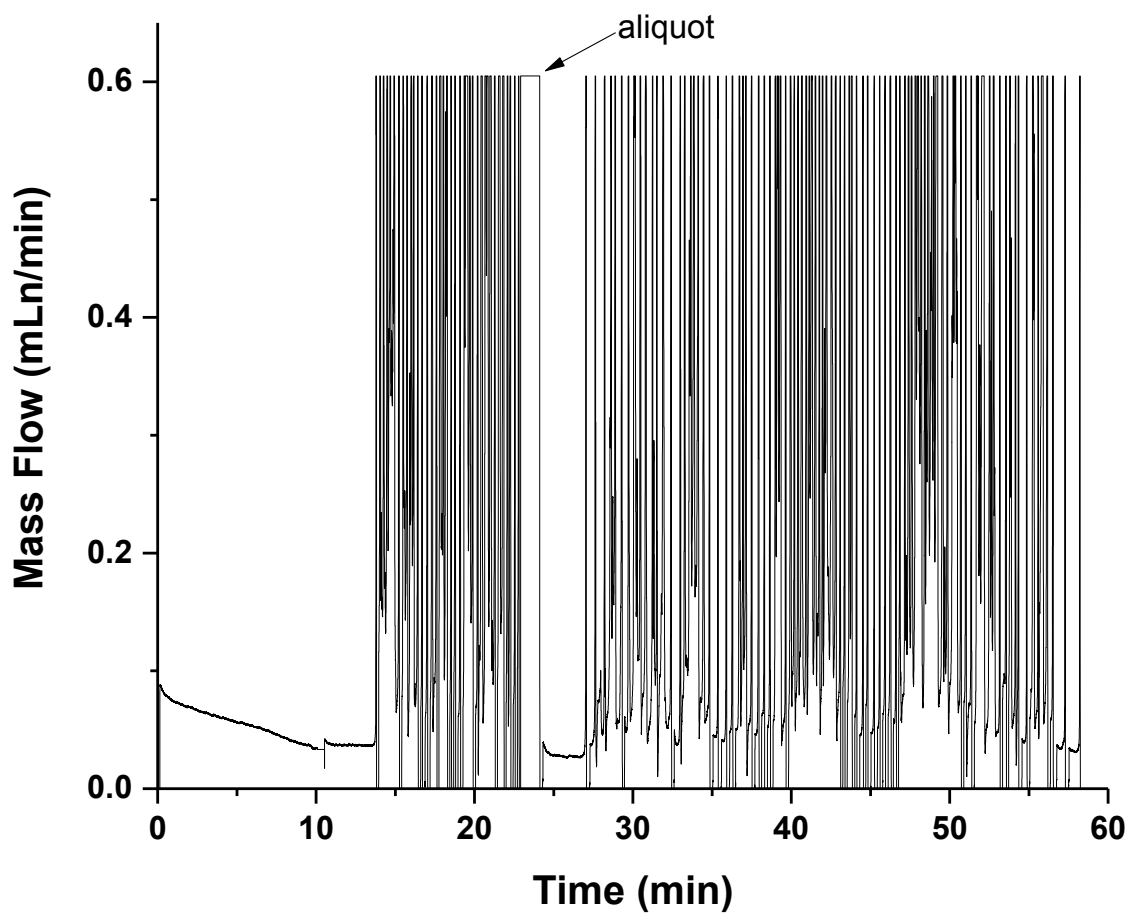


Figure S21: Mass flow of CO₂ in mLn/min for the polymerization of PA/CHO/CO₂ with catalyst 4 (Table 1, entry 8).

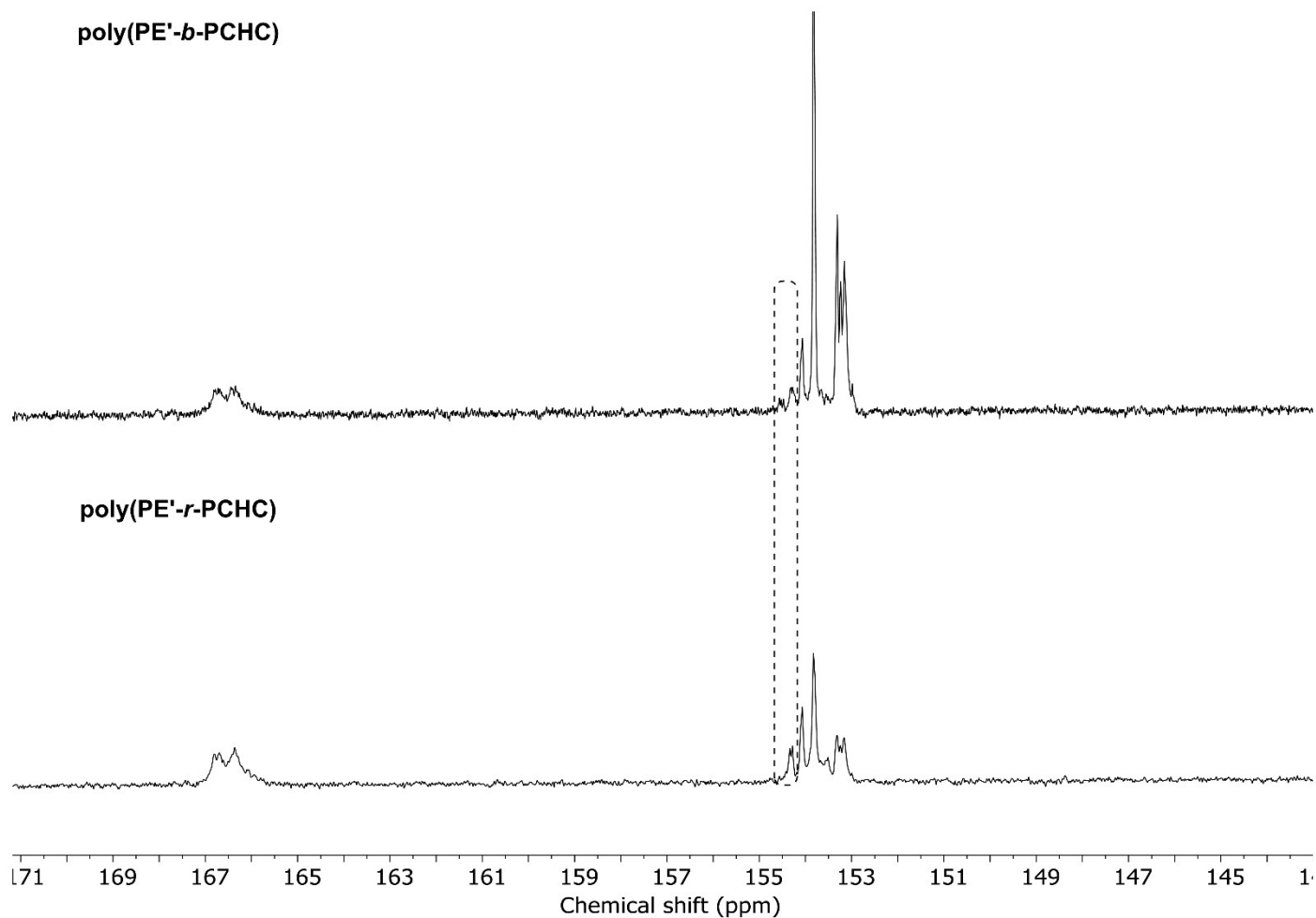


Figure S22: Selected regions of the $^{13}\text{C}\{^1\text{H}\}$ NMR spectra (125.8 MHz, CDCl_3) of poly(PE'-*b*-PCHC) (top) and poly(PE'-*r*-PCHC) (bottom). A sharper peak for the polycarbonate junction unit can be observed at 154 ppm for the random copolymer.

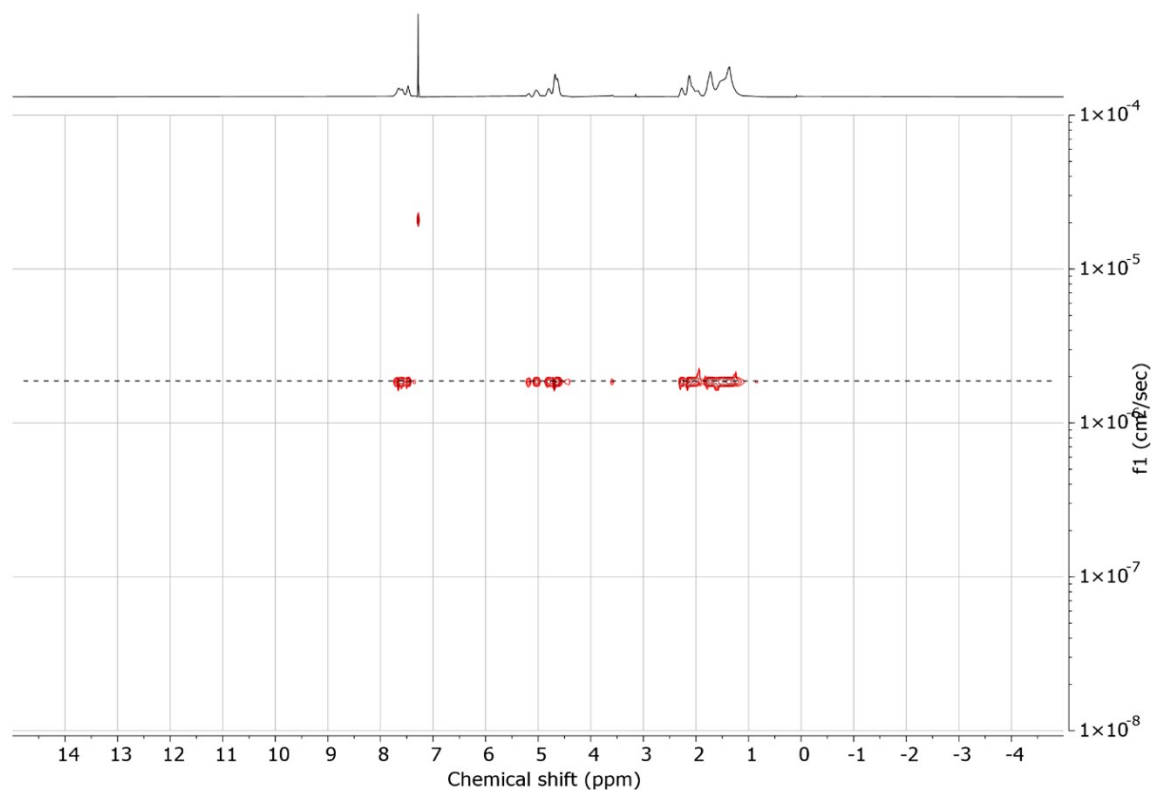


Figure S23: ^1H DOSY NMR spectrum (CDCl_3 , 500 MHz) of the purified random copolymer obtained from the polymerization of PA/CHO/ CO_2 with catalyst 4.

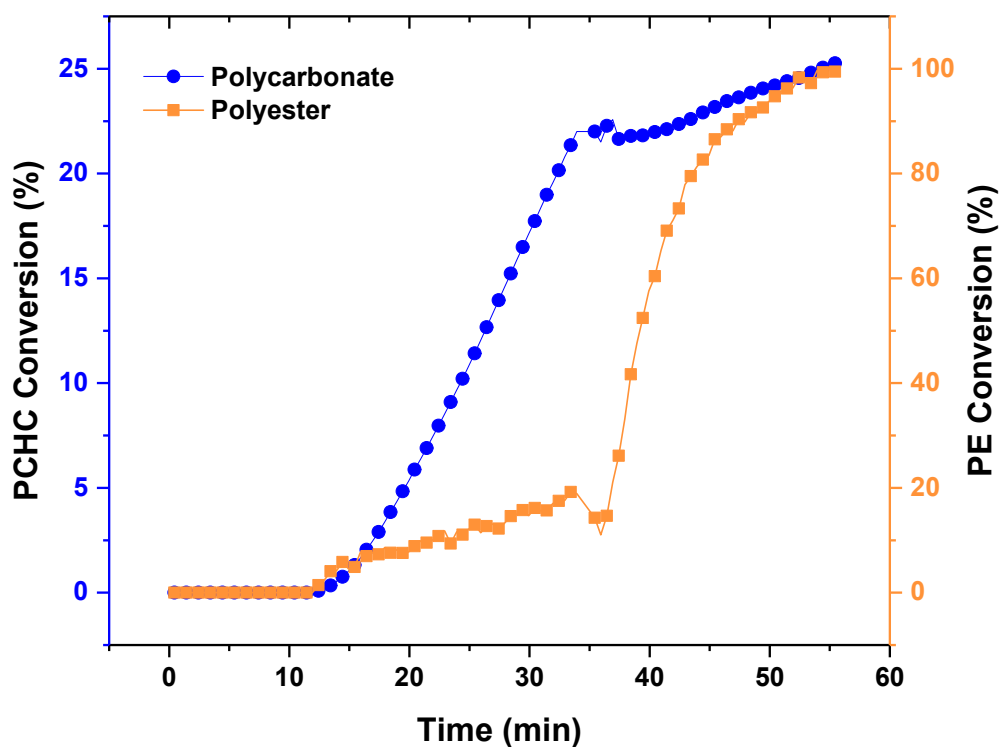


Figure S24: Conversion vs time plot using data from ATR-IR spectroscopy for the polymerization of PA/CHO/CO₂ at 20 bar of CO₂ with catalyst **4**.

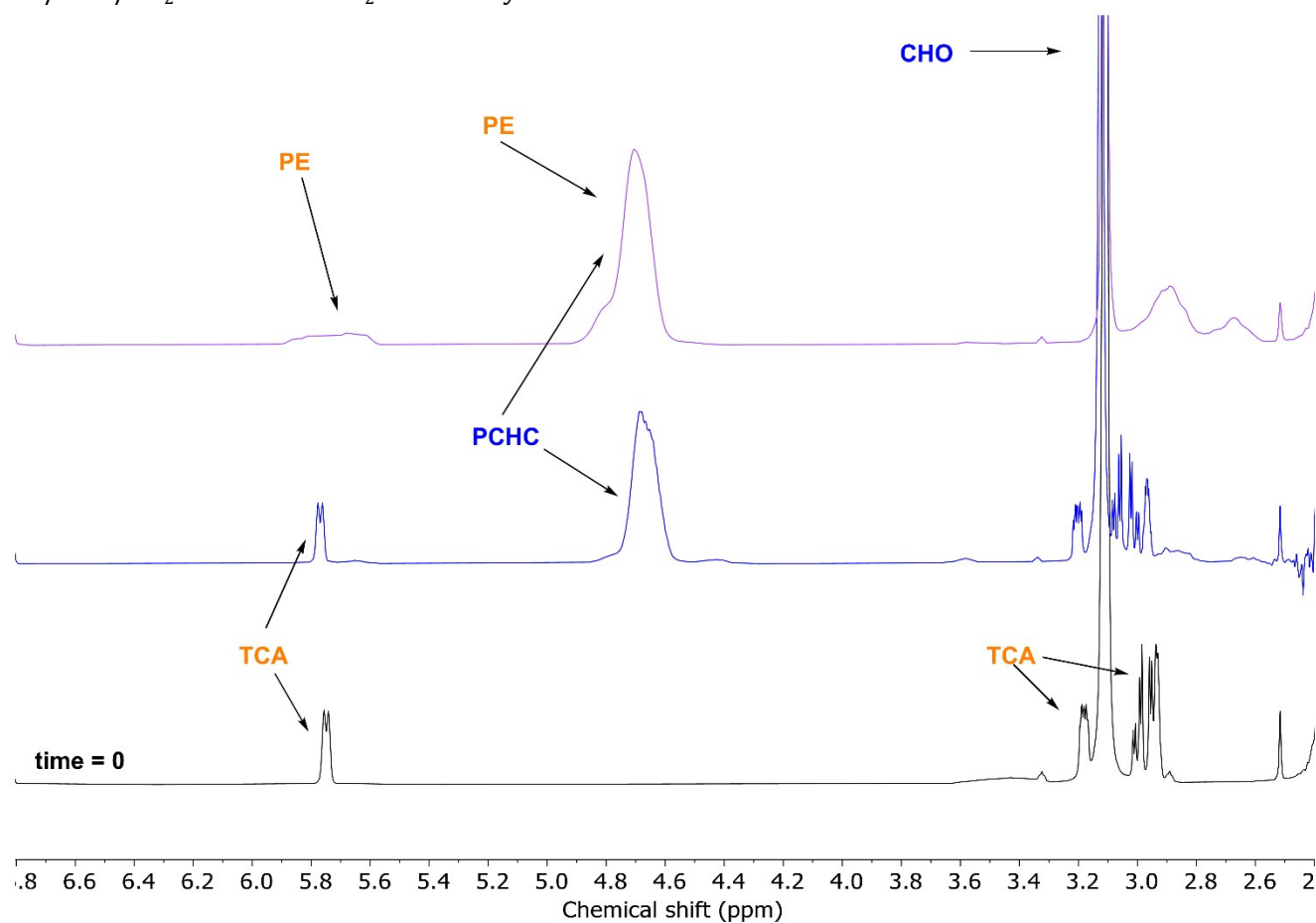


Figure S25: ¹H NMR spectra (CDCl₃, 400 MHz) of aliquots taken during the polymerization of PA/CHO/CO₂ (20 bar) with catalyst **4** (Table 1, entry 9). Bottom spectrum: after 35 min under 20 bar of CO₂. Top spectrum: after 20 min under air.

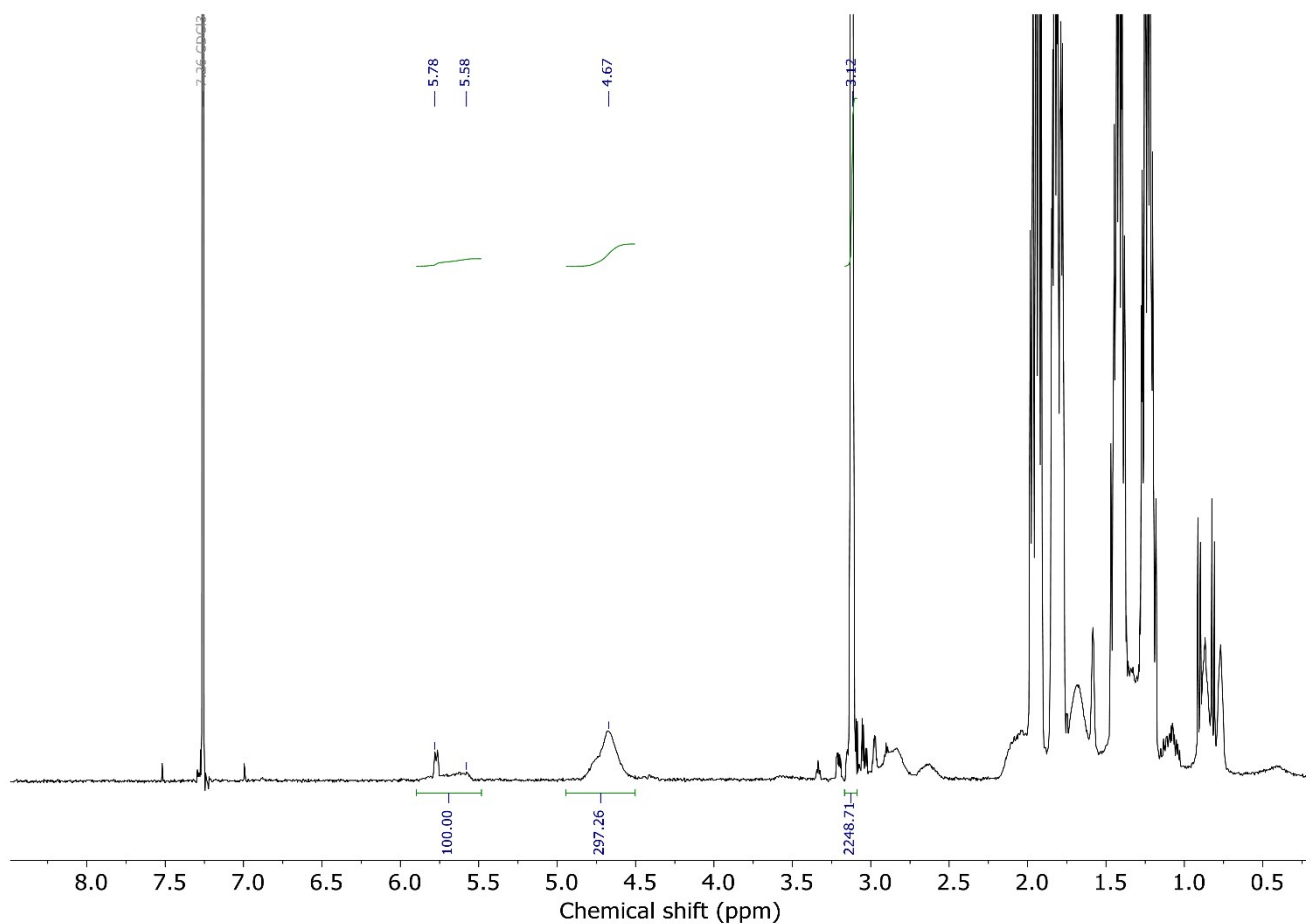


Figure S26: Example ^1H NMR spectrum (CDCl_3 , 400 MHz) showing resonances and integrals for a typical TCA/CHO/ CO_2 ROCOP.

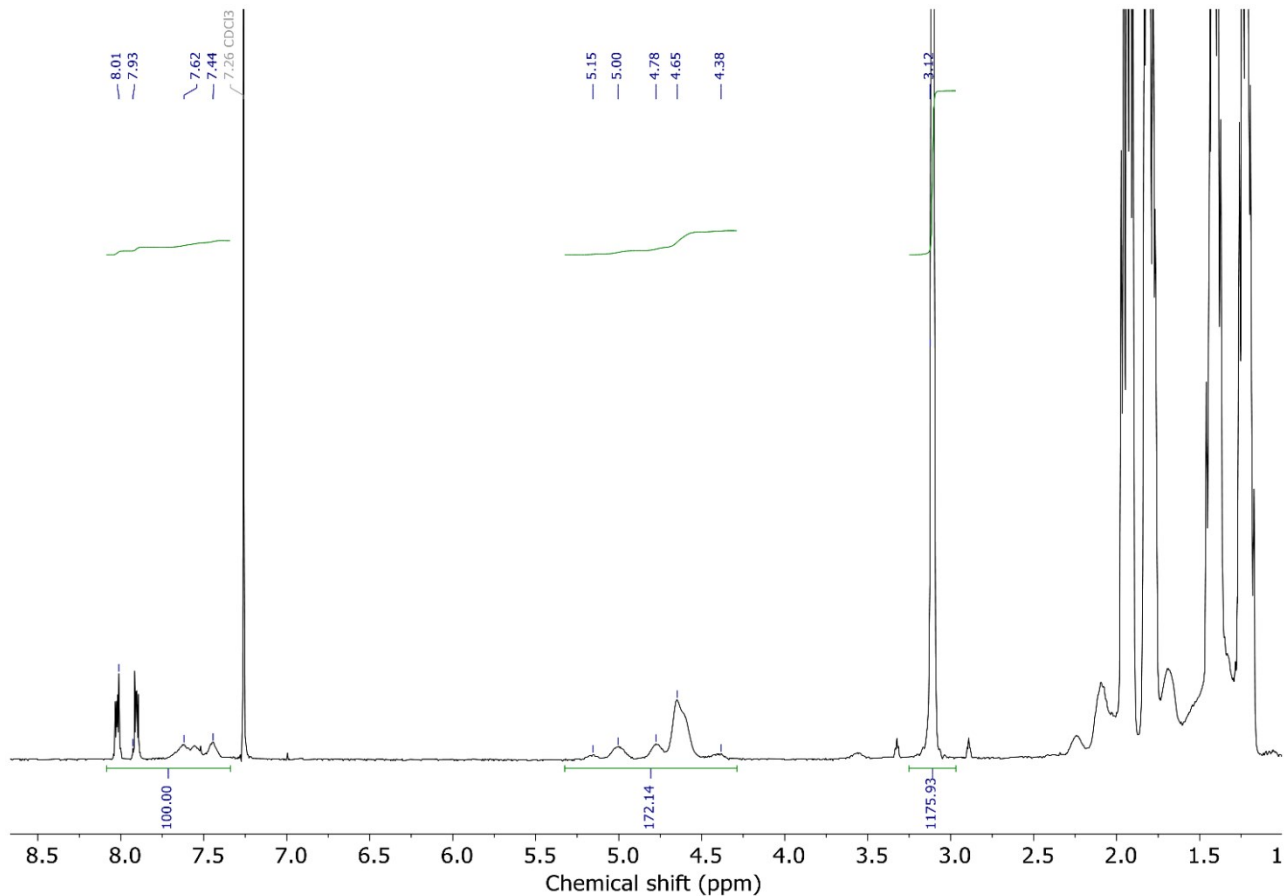


Figure S27: Example ^1H NMR spectrum (CDCl_3 , 400 MHz) showing resonances and integrals for a typical PA/CHO/ CO_2 ROCOP.

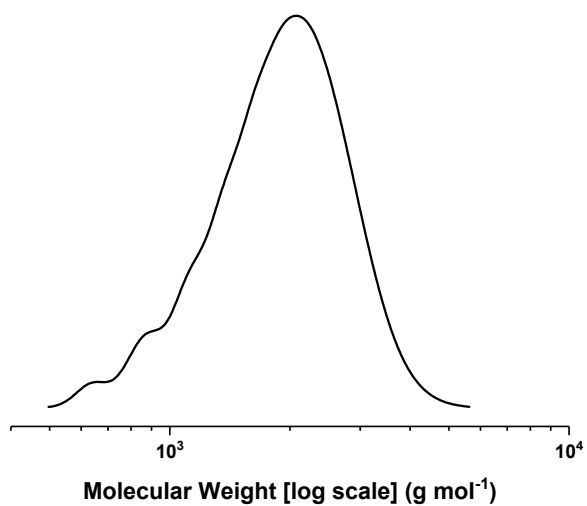


Figure S28: GPC plot of M_n for catalyst **1** TCA/CHO at 1 bar CO_2 (Table 1, entry 1)

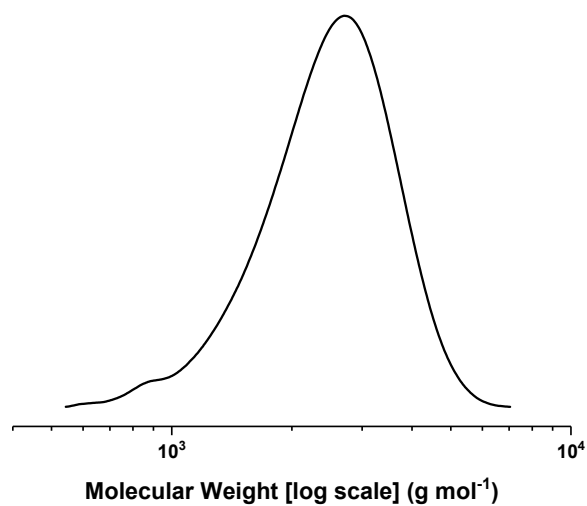


Figure S29: GPC plot of M_n for catalyst **2** TCA/CHO at 1 bar CO_2 (Table 1, entry 2)

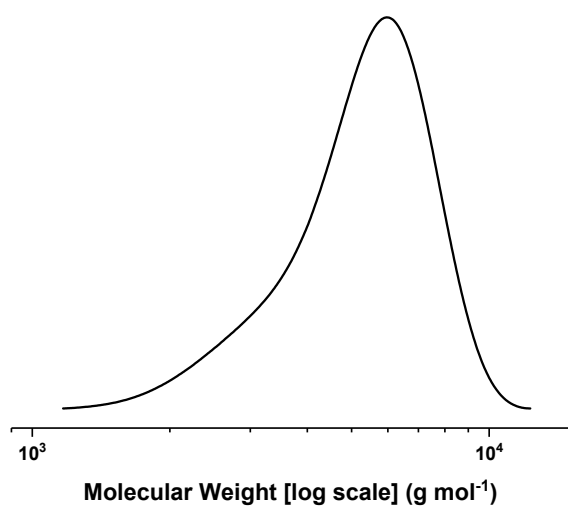


Figure S30: GPC plot of M_n for catalyst **3** TCA/CHO at 1 bar CO_2 (Table 1, entry 3)

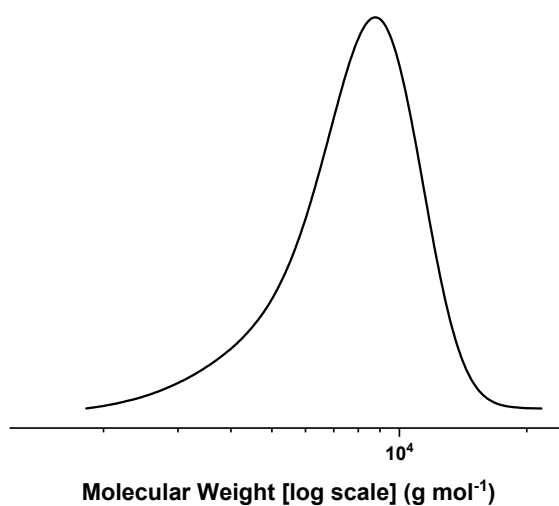


Figure S31: GPC plot of M_n for catalyst **4** TCA/CHO at 1 bar CO_2 (Table 1, entry 4)

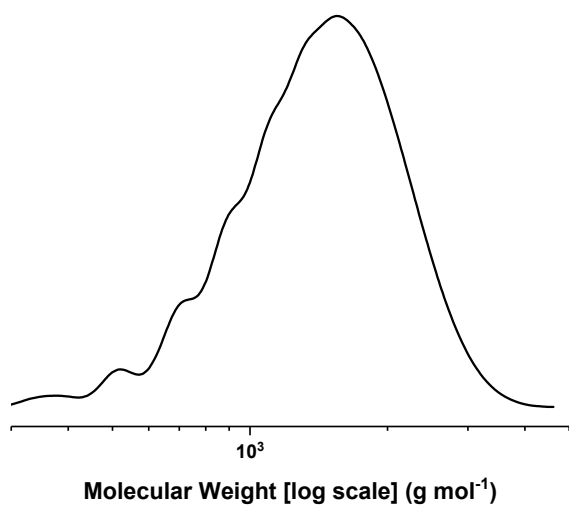


Figure S32: GPC plot of M_n for catalyst 1 PA/CHO at 1 bar CO_2 (Table 1, entry 5)

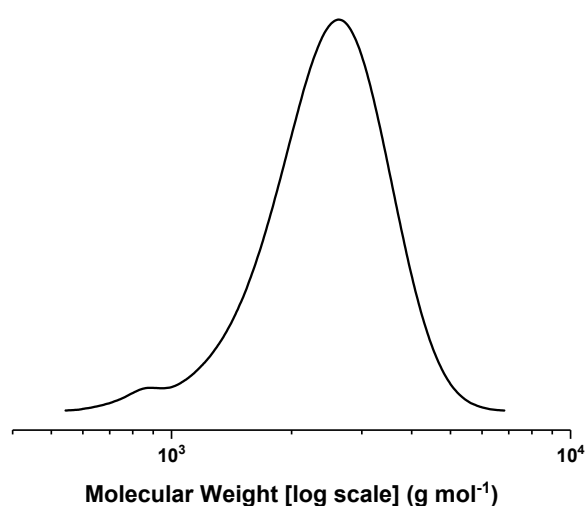


Figure S33: GPC plot of M_n for catalyst 2 PA/CHO at 1 bar CO_2 (Table 1, entry 6)

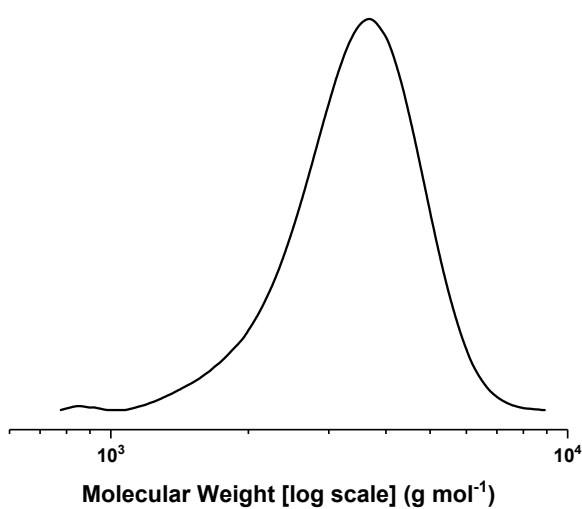


Figure S34: GPC plot of M_n for catalyst 3 PA/CHO at 1 bar CO_2 (Table 1, entry 7)

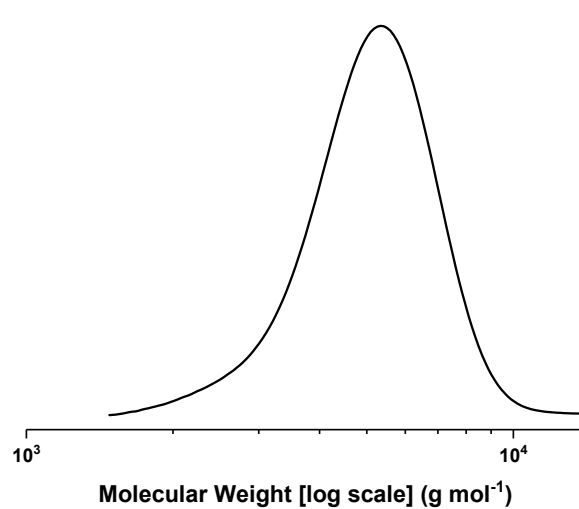


Figure S35: GPC plot of M_n for catalyst 4 PA/CHO at 1 bar CO_2 (Table 1, entry 8)

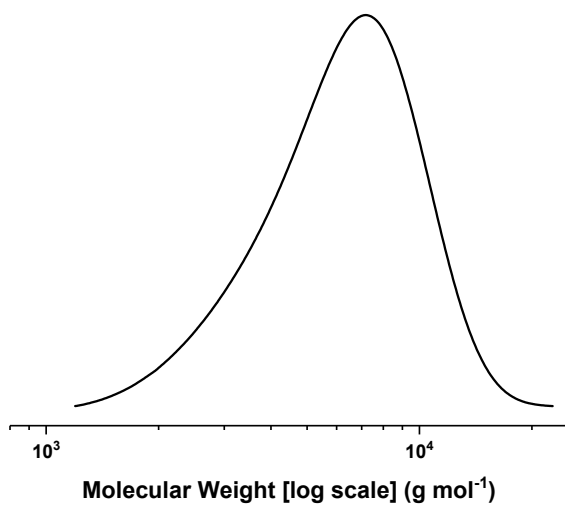


Figure S36: GPC plot of M_n for catalyst 4 PA/CHO at 20 bar CO_2 (Table 1, entry 9)

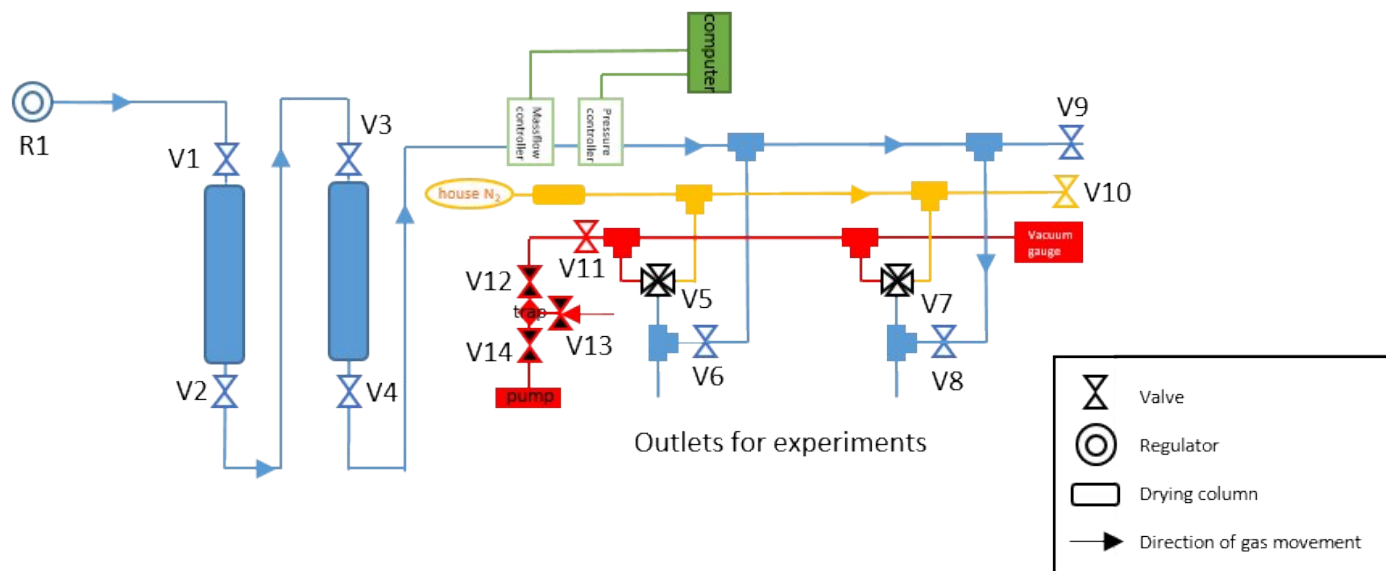


Figure S37: Diagram of the steel triple manifold Schlenk line used to reversibly switch between CO₂, N₂, and vacuum.

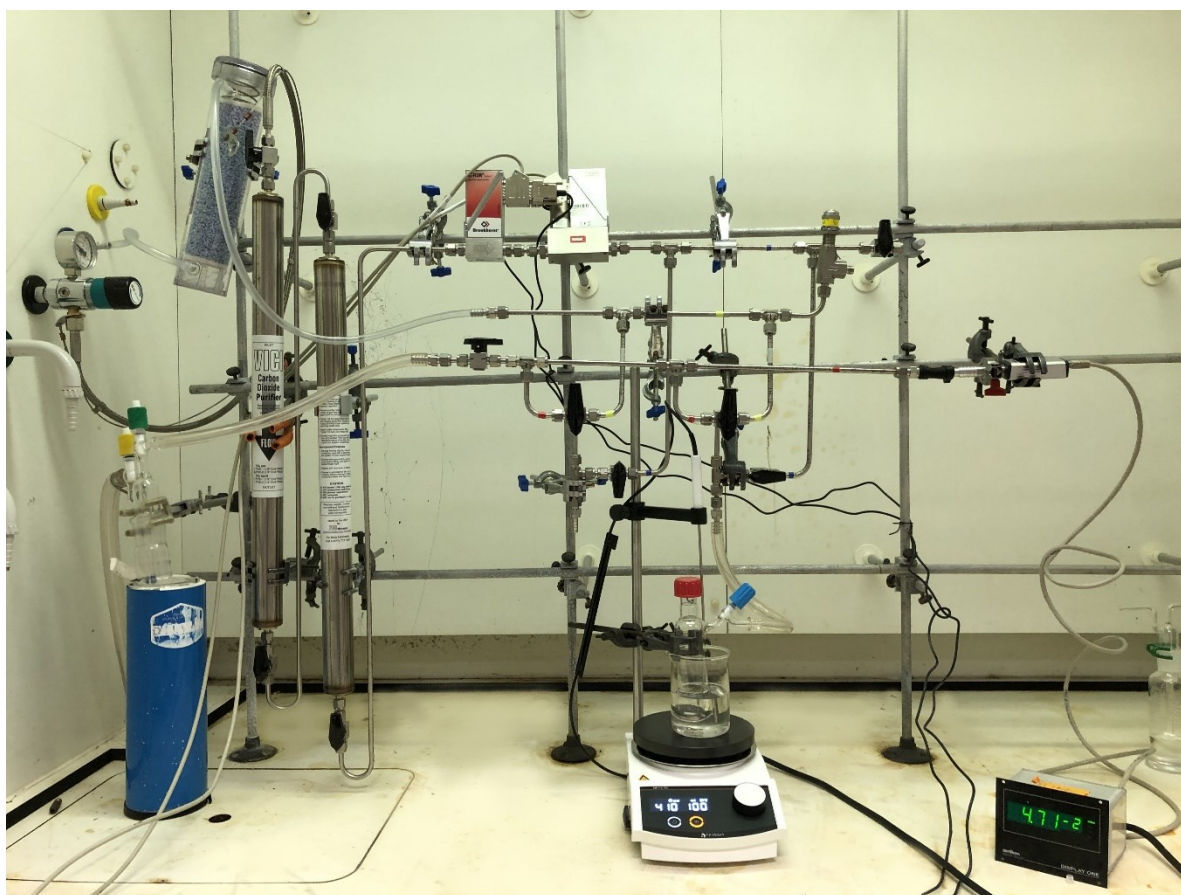


Figure S38: Photograph of the steel triple manifold Schlenk line. CO₂ pressure is regulated and controlled with a Bronkhorst pressure controller, such that when the pressure drops below the set pressure (due to CO₂ consumption), the system is automatically pressurized. Mass flow measurements can be recorded using the mass flow metre.

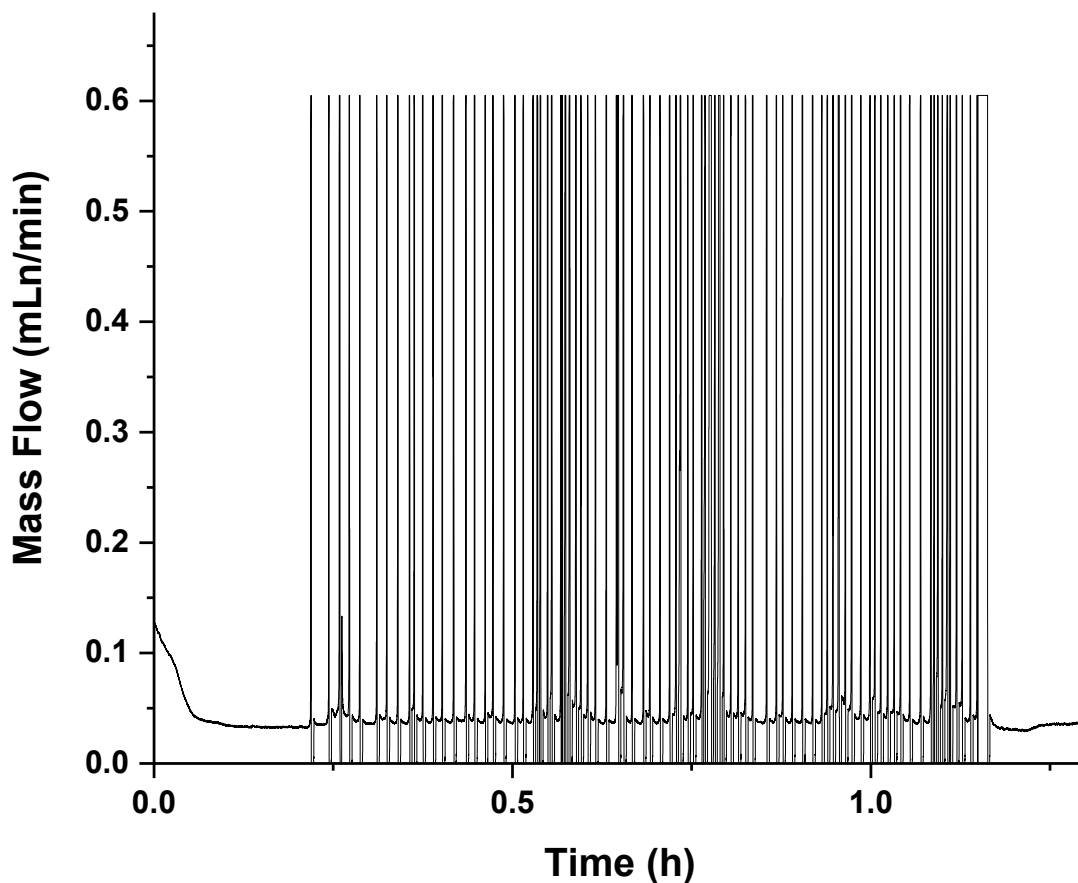


Figure S39: Example raw data from the mass flow controller, showing the periodic increase in CO₂ mass flow as CO₂ is being consumed throughout the reaction.

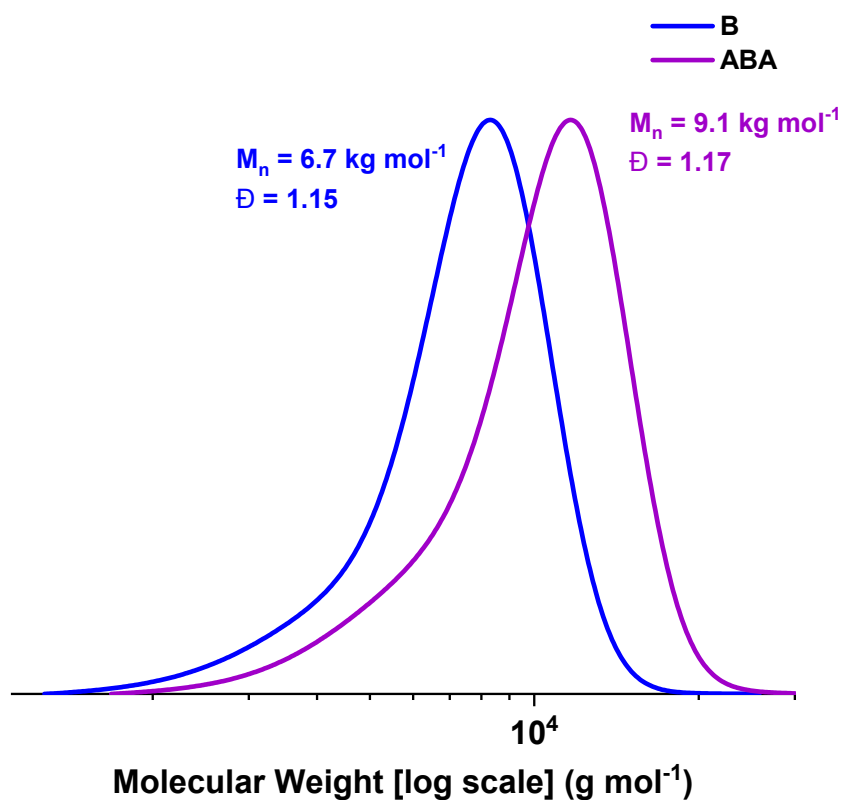


Figure S40: GPC traces illustrating the increase in molecular weight with block formation during the polymerization with one CO₂/N₂ gas switches (Table 2, entry 1).

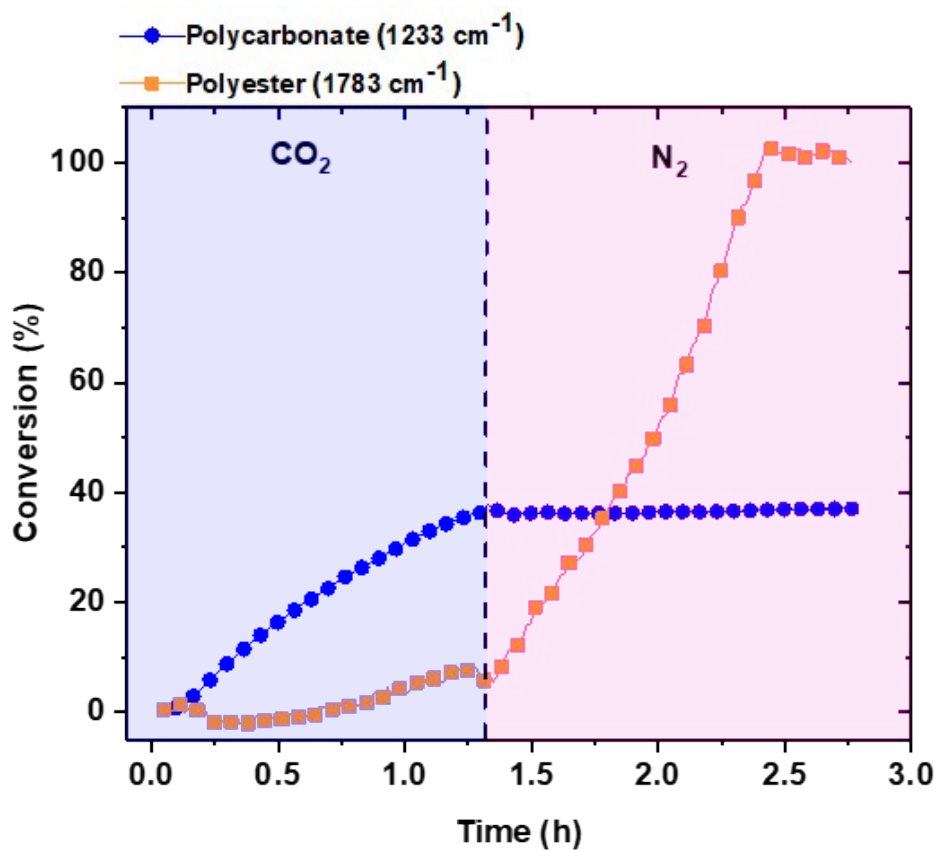


Figure S41: Conversion vs time plot using data from ATR-IR spectroscopy for the polymerization of TCA/CHO/CO₂ with catalyst 4, which was switched to a N₂ atmosphere after 1.3 h. Note that the signal for polyester formation between 0 – 1.3 h apparently increases due to signal overlap with the growing polycarbonate (no conversion to polyester was observed by ¹H NMR spectroscopy).

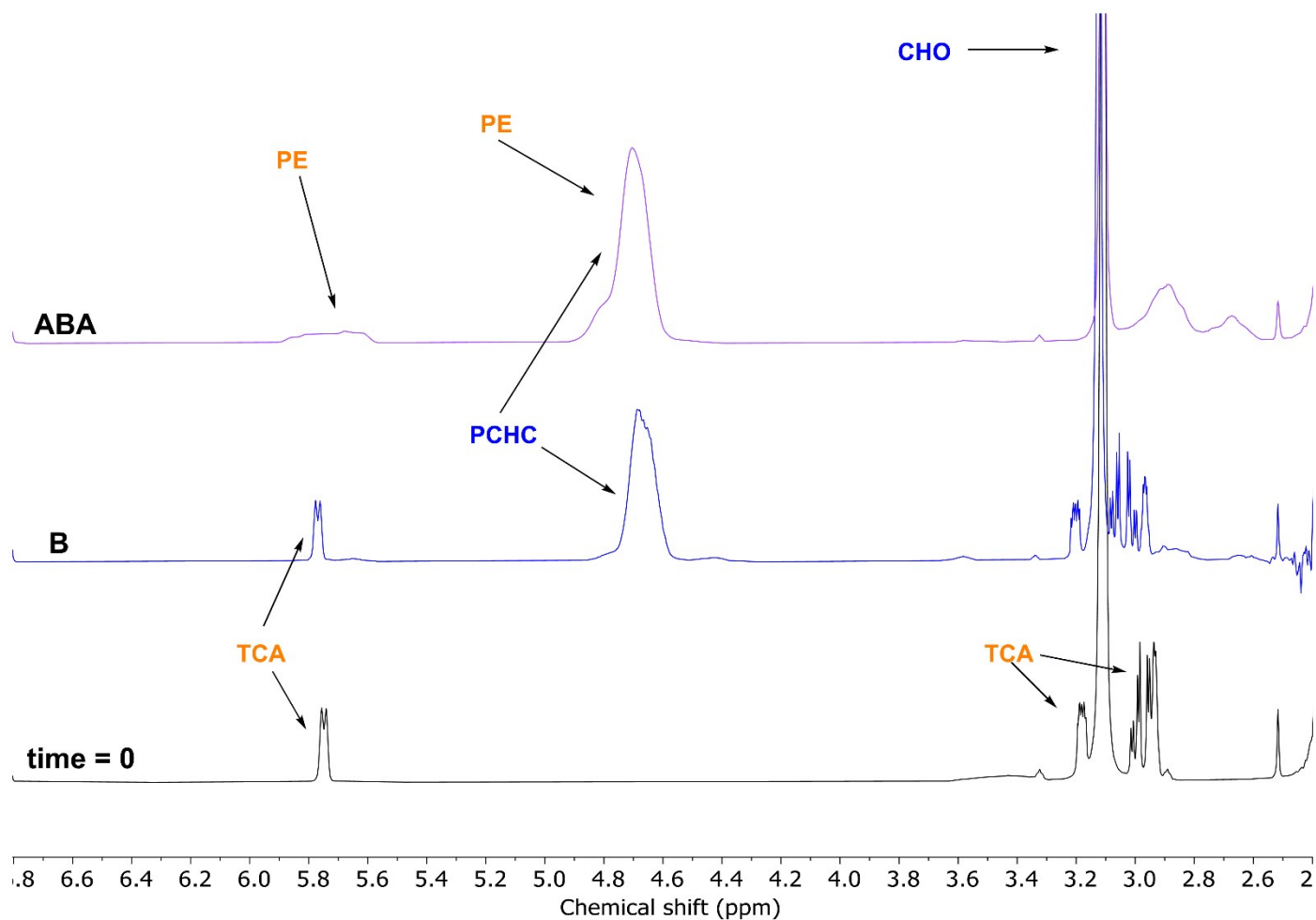


Figure S42: Selected regions of ^1H NMR spectra of reaction aliquots illustrating the changes in resonances during the different stages of the ABA triblock formation (Table 2, entry 1).

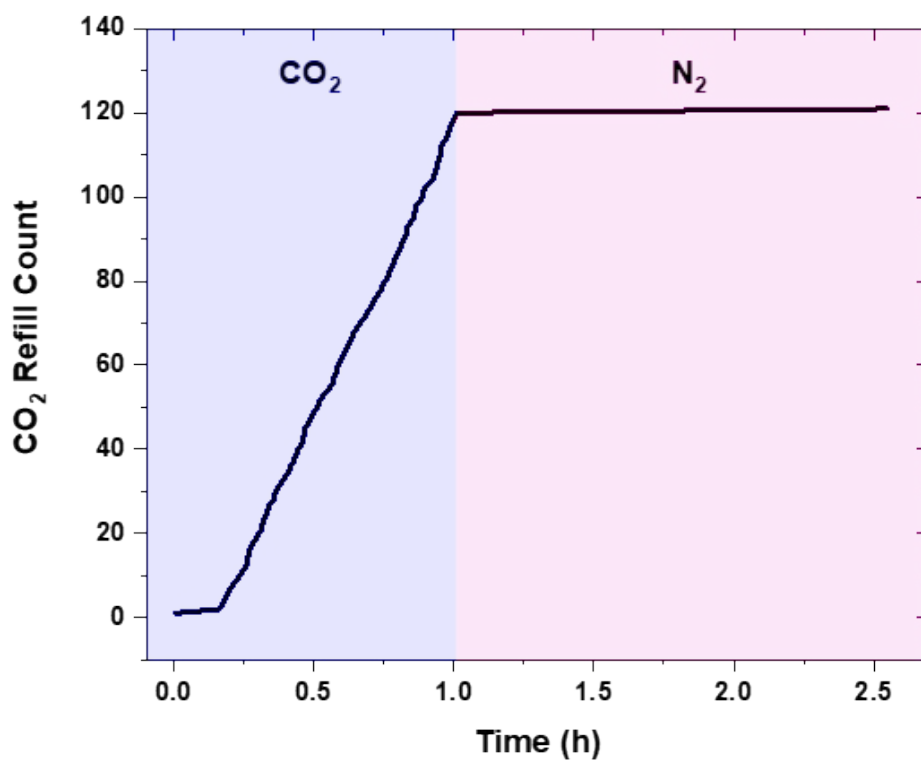


Figure S43: Frequency of CO_2 flow extracted from mass flow data for the polymerization in Table 2, entry 1, which was switched to a N_2 atmosphere after 1 h.

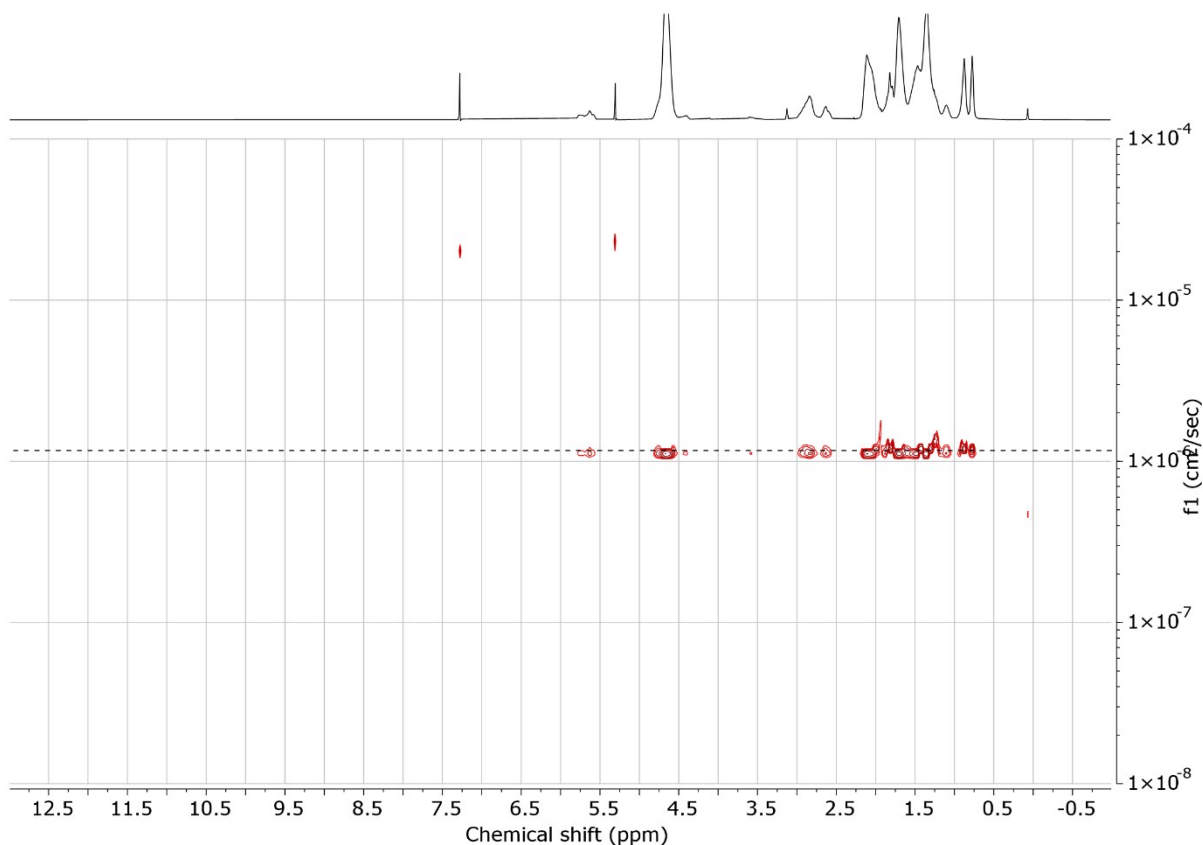


Figure S44: ^1H DOSY NMR spectrum (CDCl_3 , 500 MHz) of the purified ABA triblock.

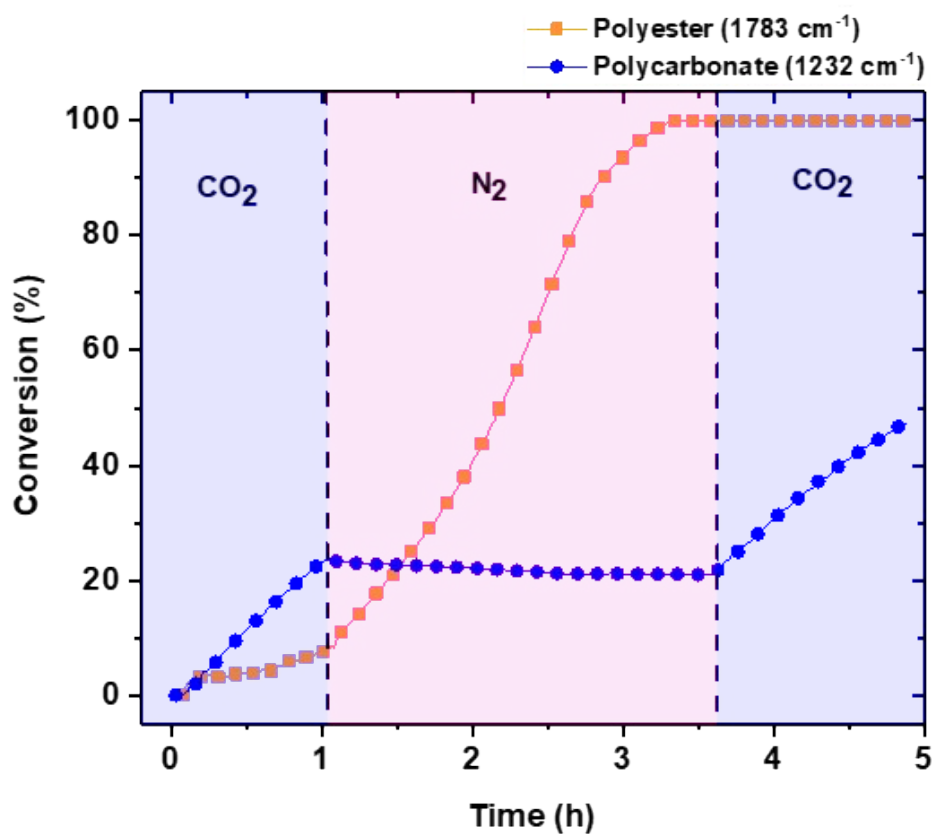


Figure S45: Conversion vs time plot using data from ATR-IR spectroscopy for the polymerization of TCA/CHO/ CO_2 with catalyst **4**, which was switched to a N_2 atmosphere after 1 h and back to CO_2 after 2.3 h under N_2 (Table 2, entry 2).

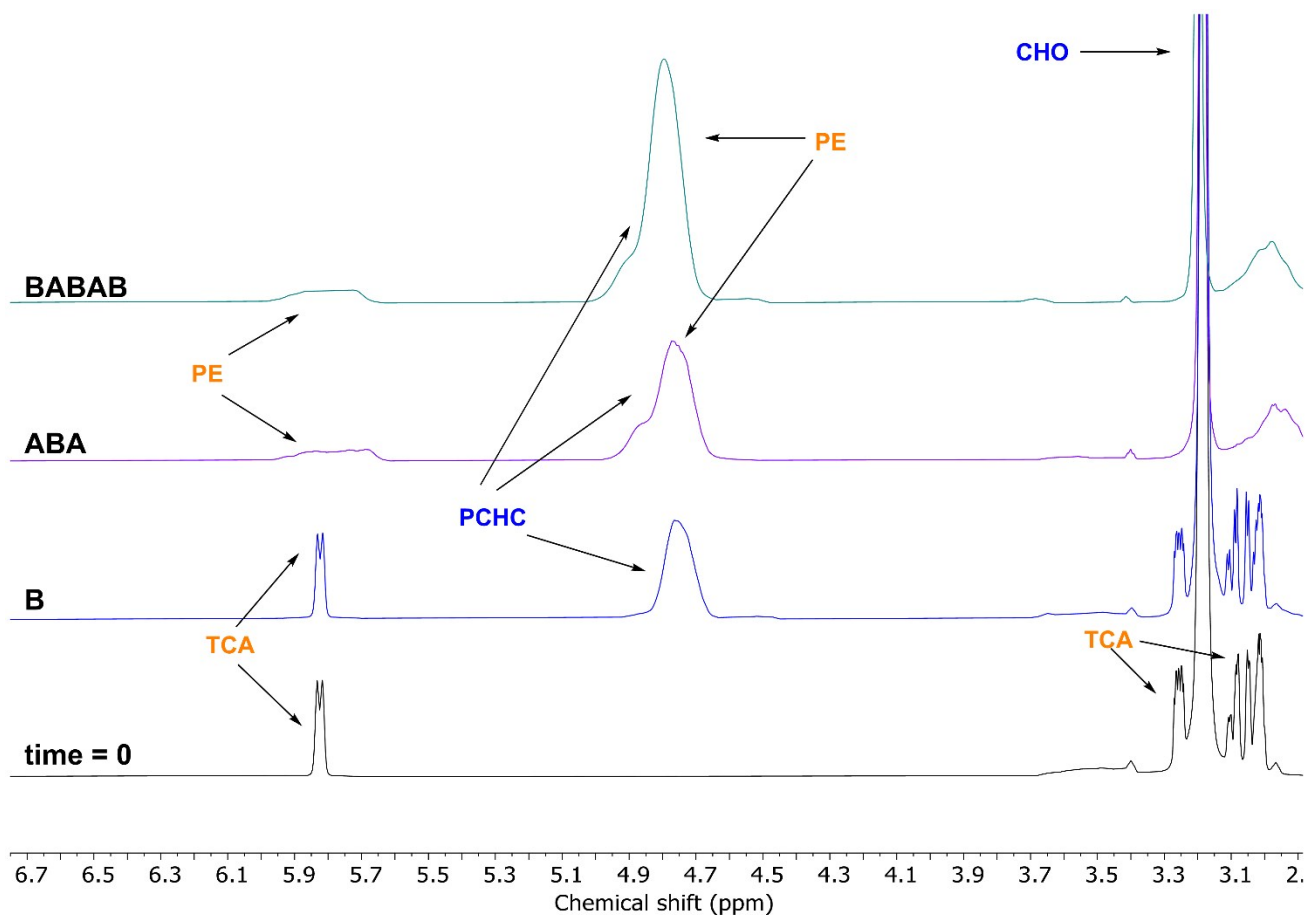


Figure S46: Selected region of ^1H NMR spectra of reaction aliquots illustrating the changes in resonances during the different stages of the BABAB pentablock formation (Table 2, entry 2).

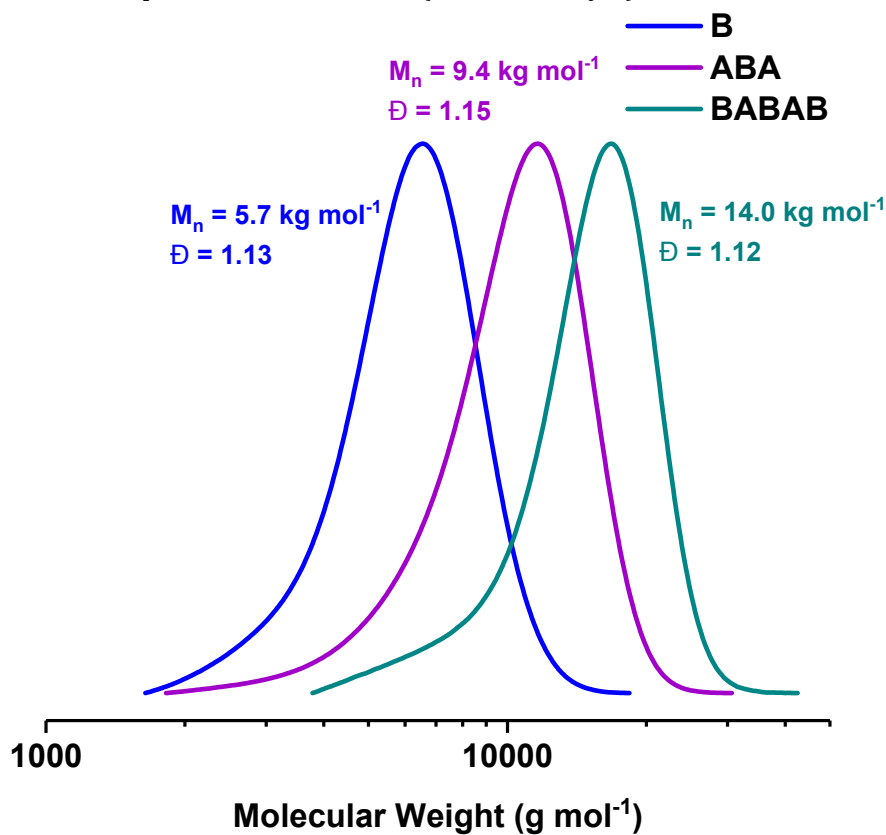


Figure S47: GPC traces illustrating the increase in molecular weight with block formation during the polymerization with two CO_2/N_2 gas switches (Table 2, entry 2).

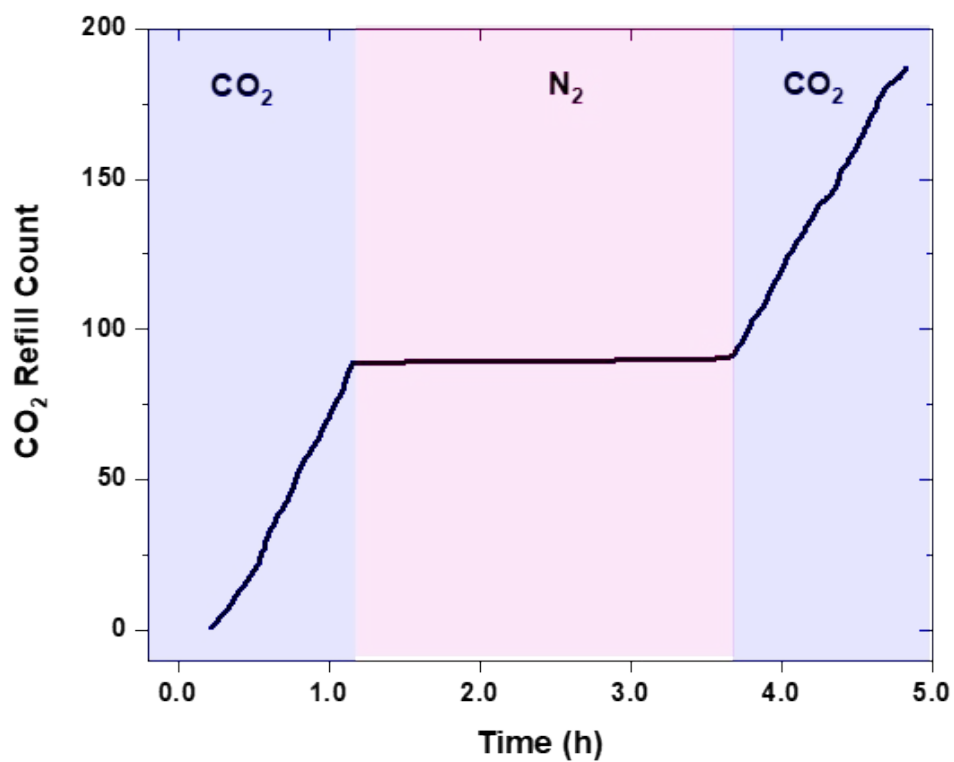


Figure S48: Frequency of CO₂ flow extracted from mass flow data for the polymerization in Table 2, entry 2, which was switched to a N₂ atmosphere after 1 h and switched back to CO₂ after 2.3 h.

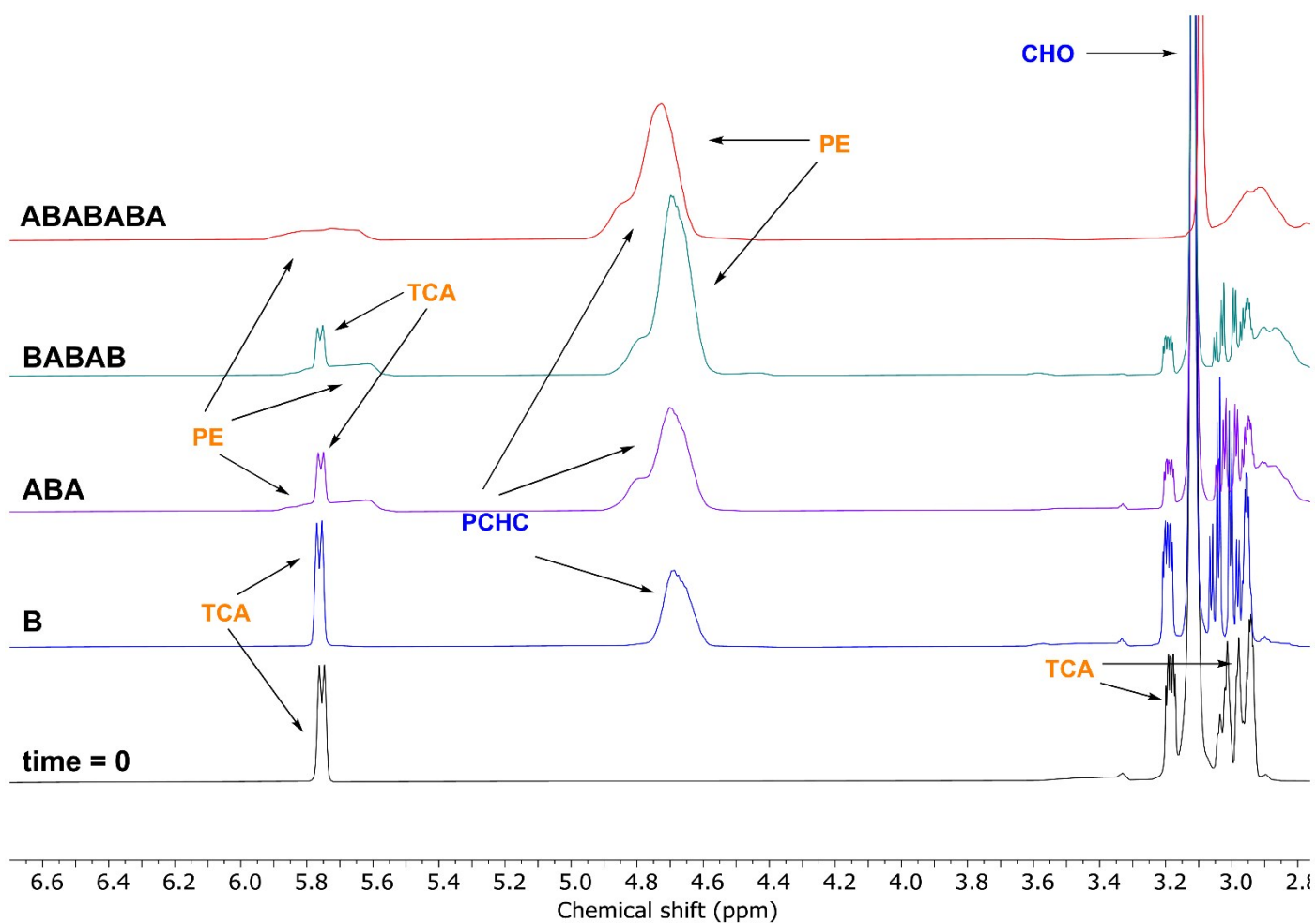


Figure S49: Selected region of ¹H NMR spectra of reaction aliquots illustrating the changes in resonances during the different stages of the ABABABA heptablock formation (Table 2, entry 3).

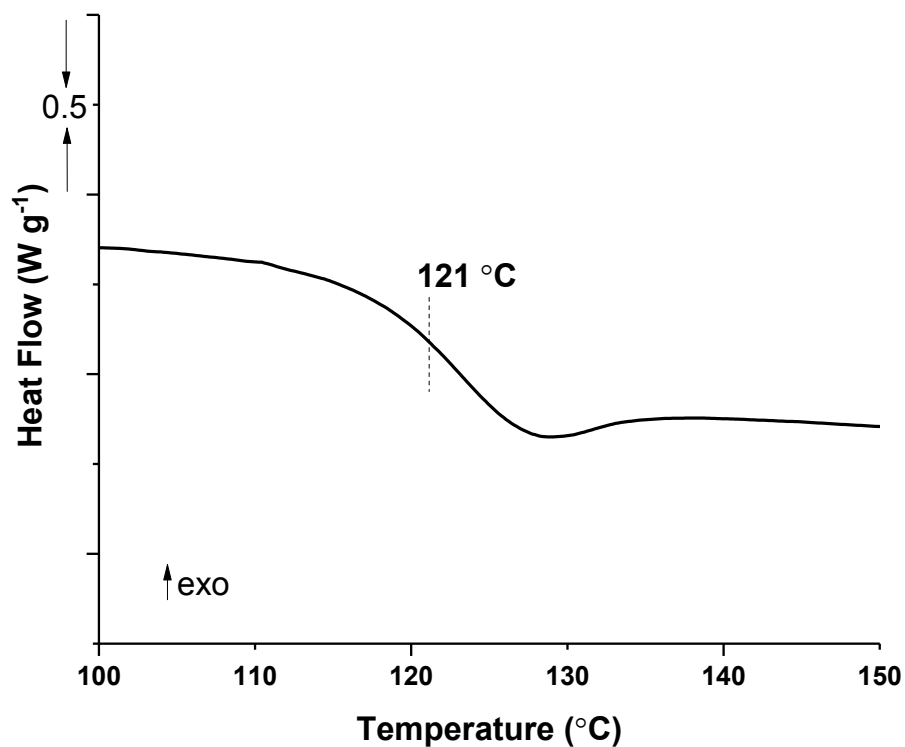


Figure S50: DSC trace of the purified ABA polymer (Table 2, entry 1).

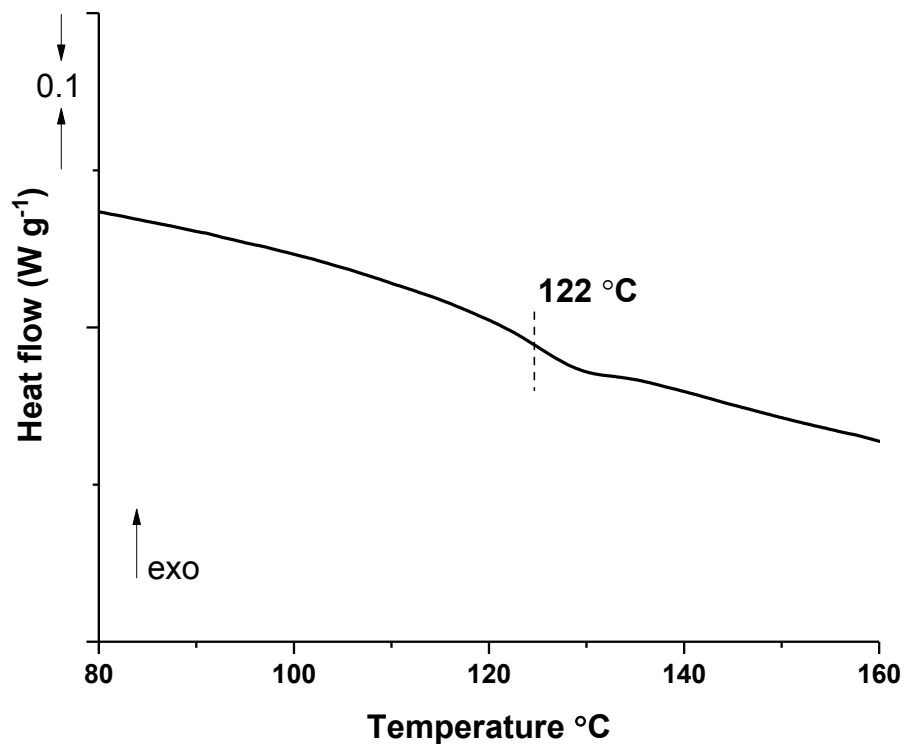


Figure S51: DSC trace of the purified BABAB polymer (Table 2, entry 2).

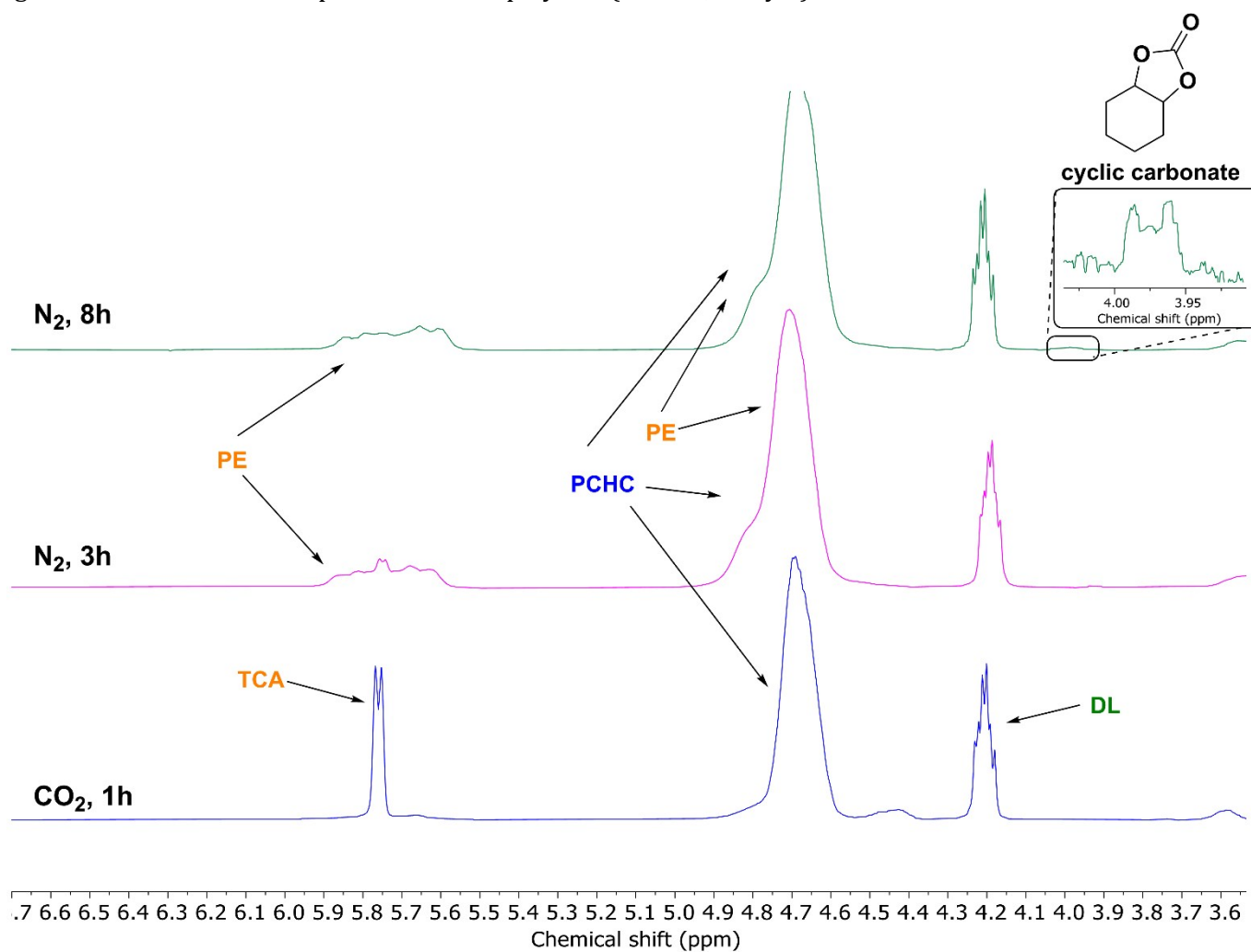


Figure S52: Selected region of the ^1H NMR spectra of reaction aliquots illustrating the changes in resonances during the different stages of the CHO/TCA/ CO_2 /DL polymerization.

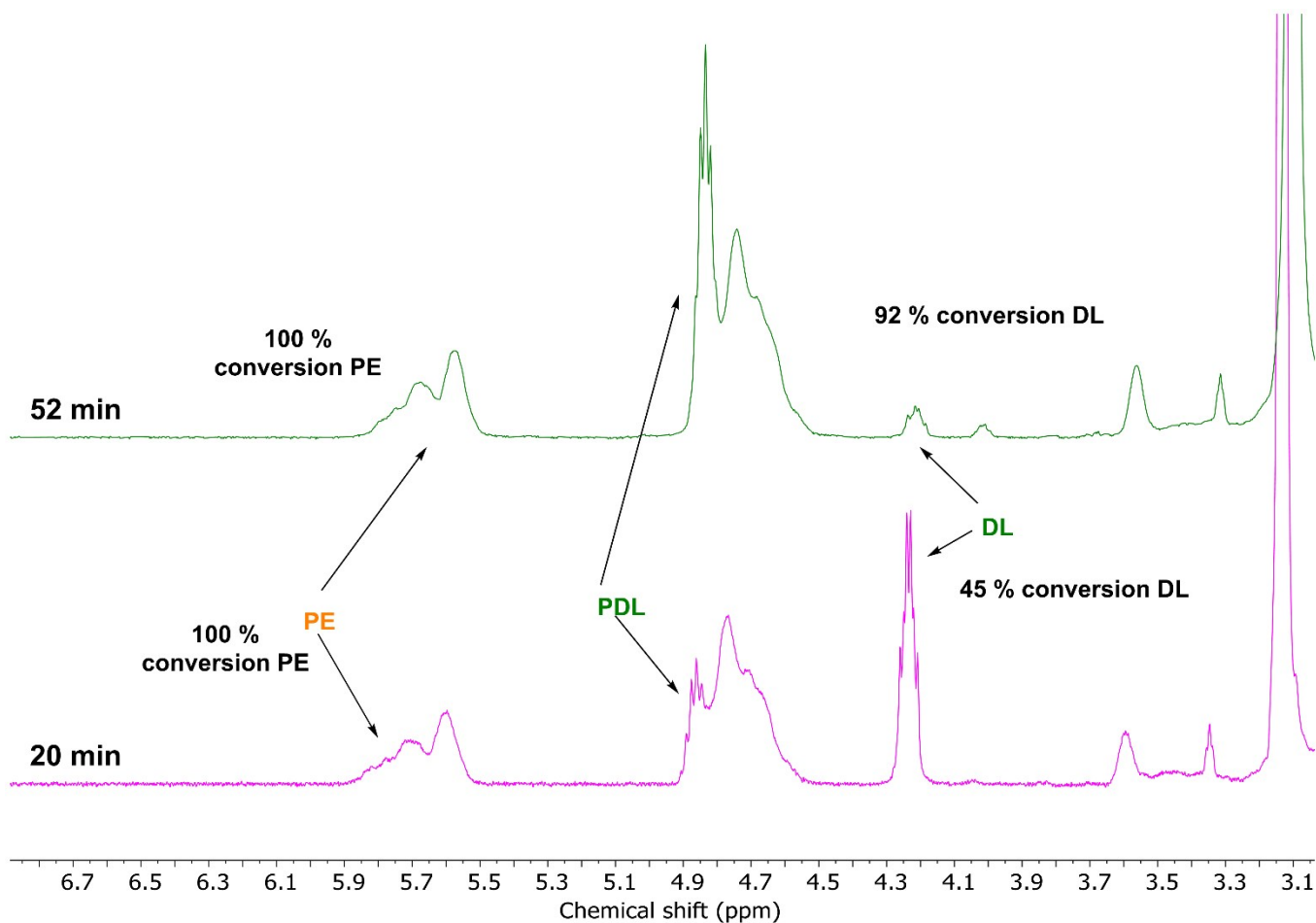


Figure S53: Selected region of the ^1H NMR spectra of reaction aliquots illustrating the changes in resonances during the different stages of the CHO/TCA/DL polymerization.

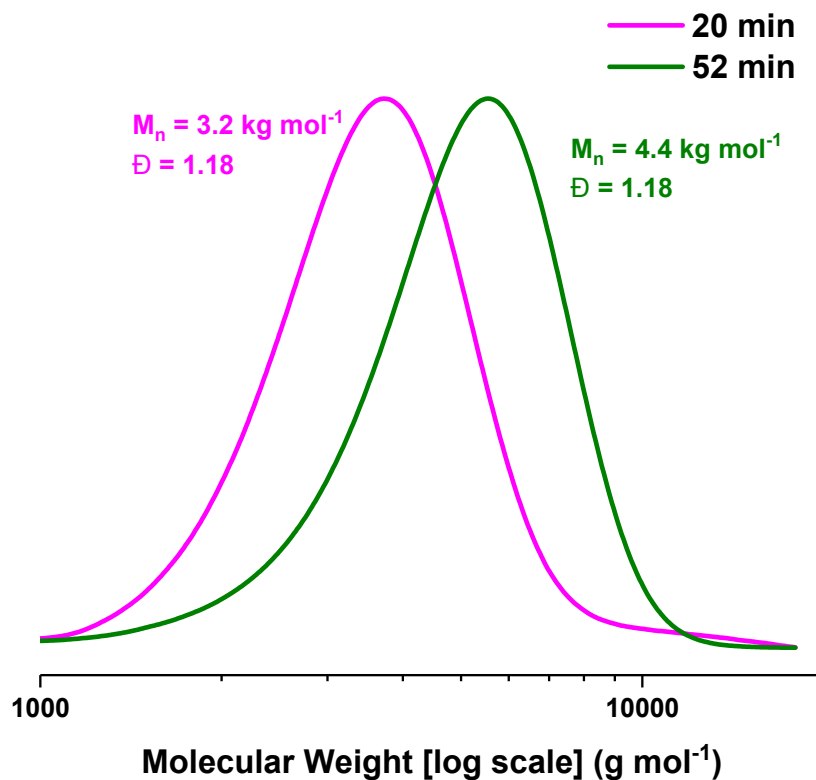


Figure S54: GPC traces corresponding to two aliquots taken for the polymerization of CHO/TCA/DL.

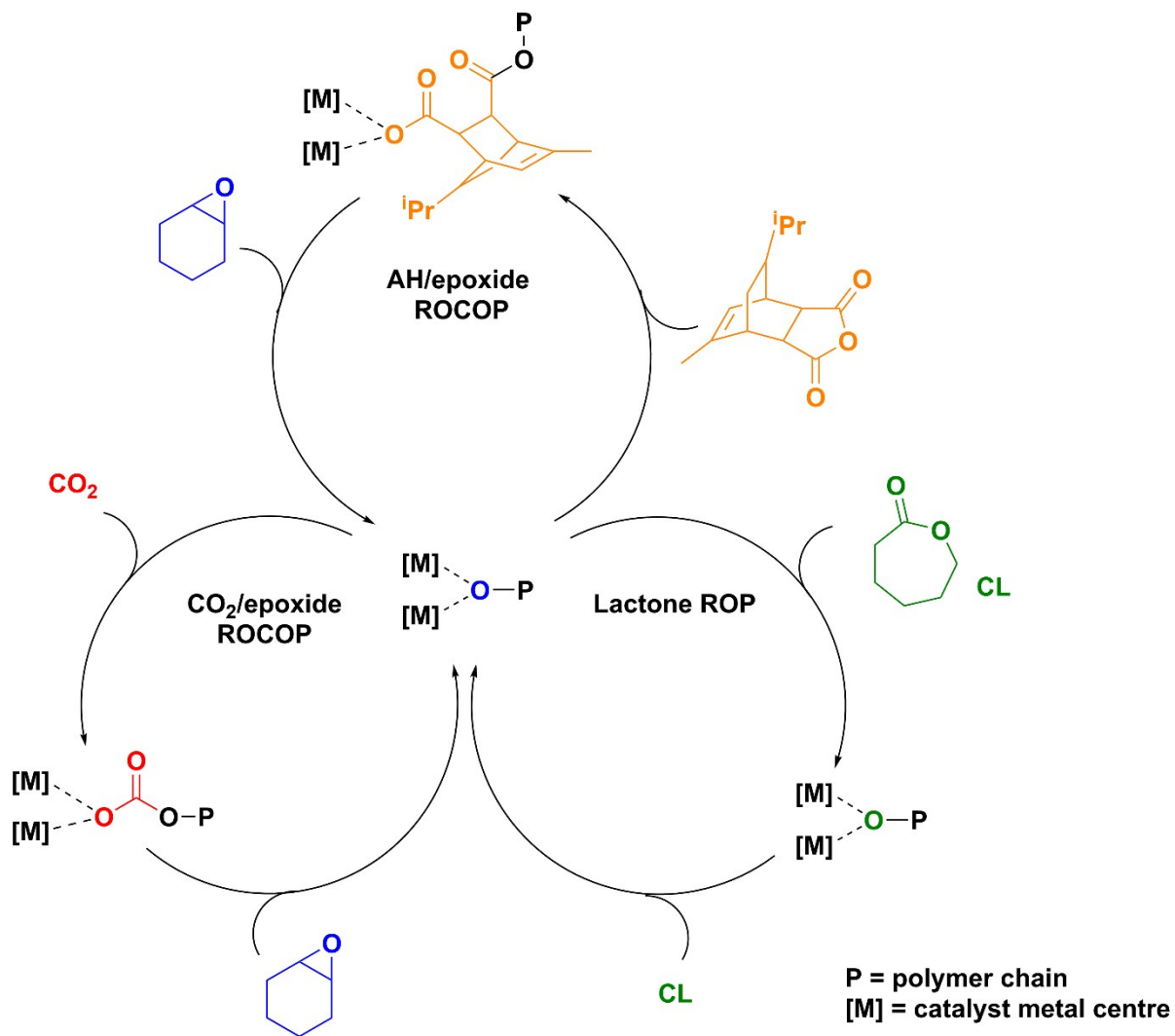


Figure S55: Catalytic cycles accessed during the switchable catalysis using CHO/CO₂/TCA/CL.

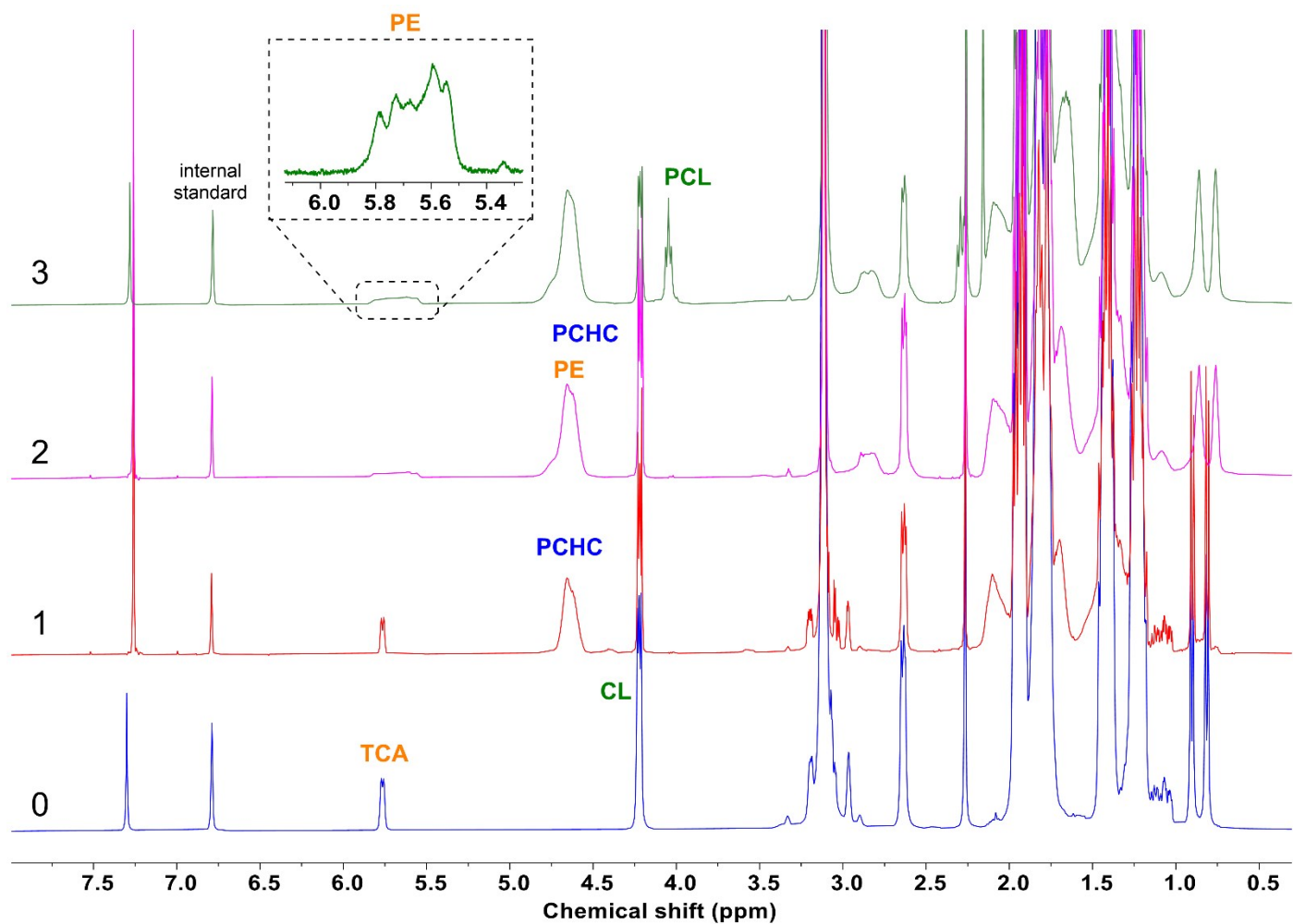


Figure S56: Stack plot showing the ¹H NMR spectra of aliquots removed during formation of the polymer blocks. Spectrum 0 is the mixture before polymerization. The first block that formed is PCHC, shown by the resonance at 4.6 ppm, the second is PE, shown by the loss of the sharp doublet into a broad polymer signal at 5.8 ppm, and the final

PCL block in 3 from the new signal at 4.0 ppm

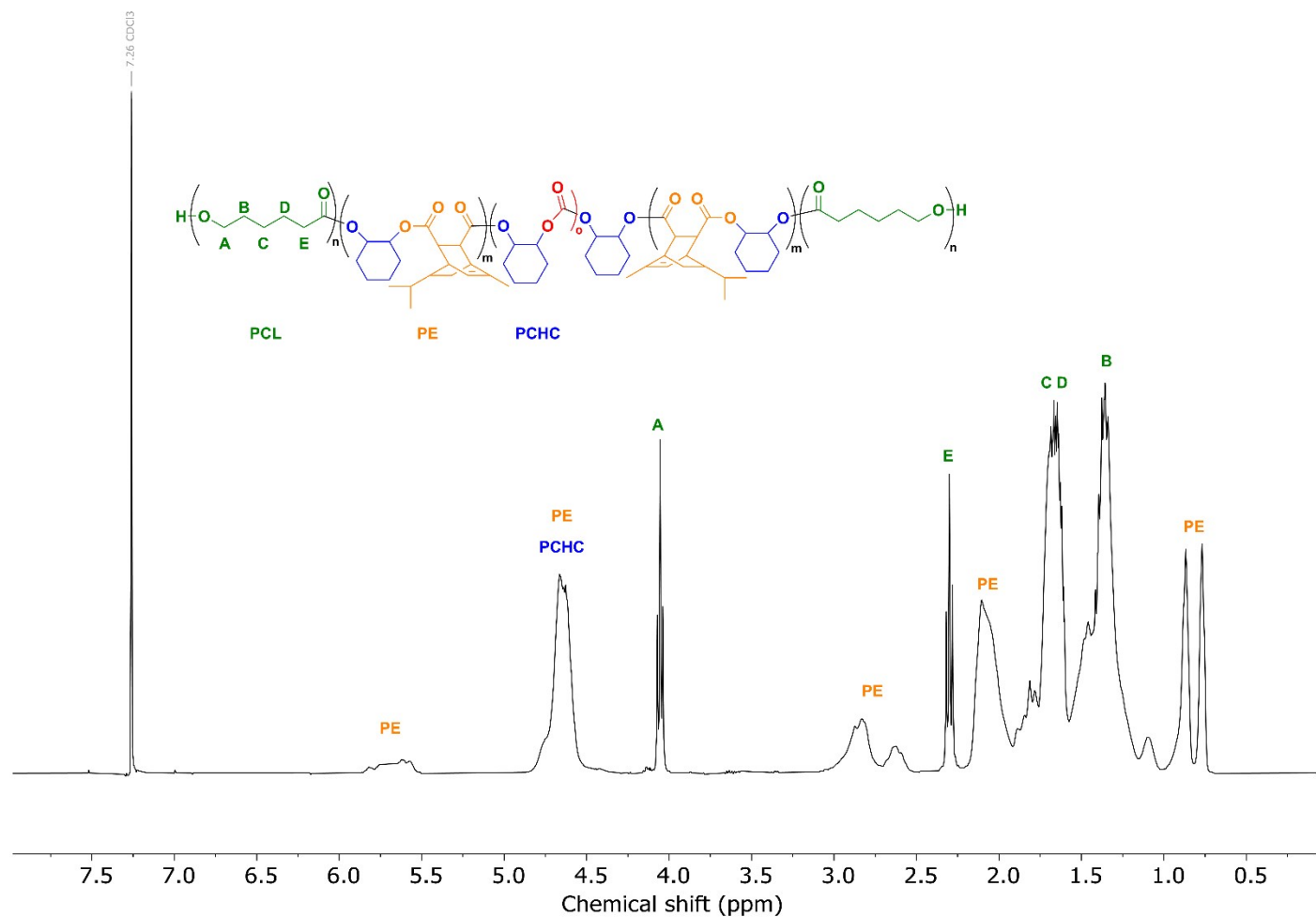


Figure S57: ¹H NMR spectrum (CDCl₃, 400 MHz) of the purified multiblock polymer CABAC.

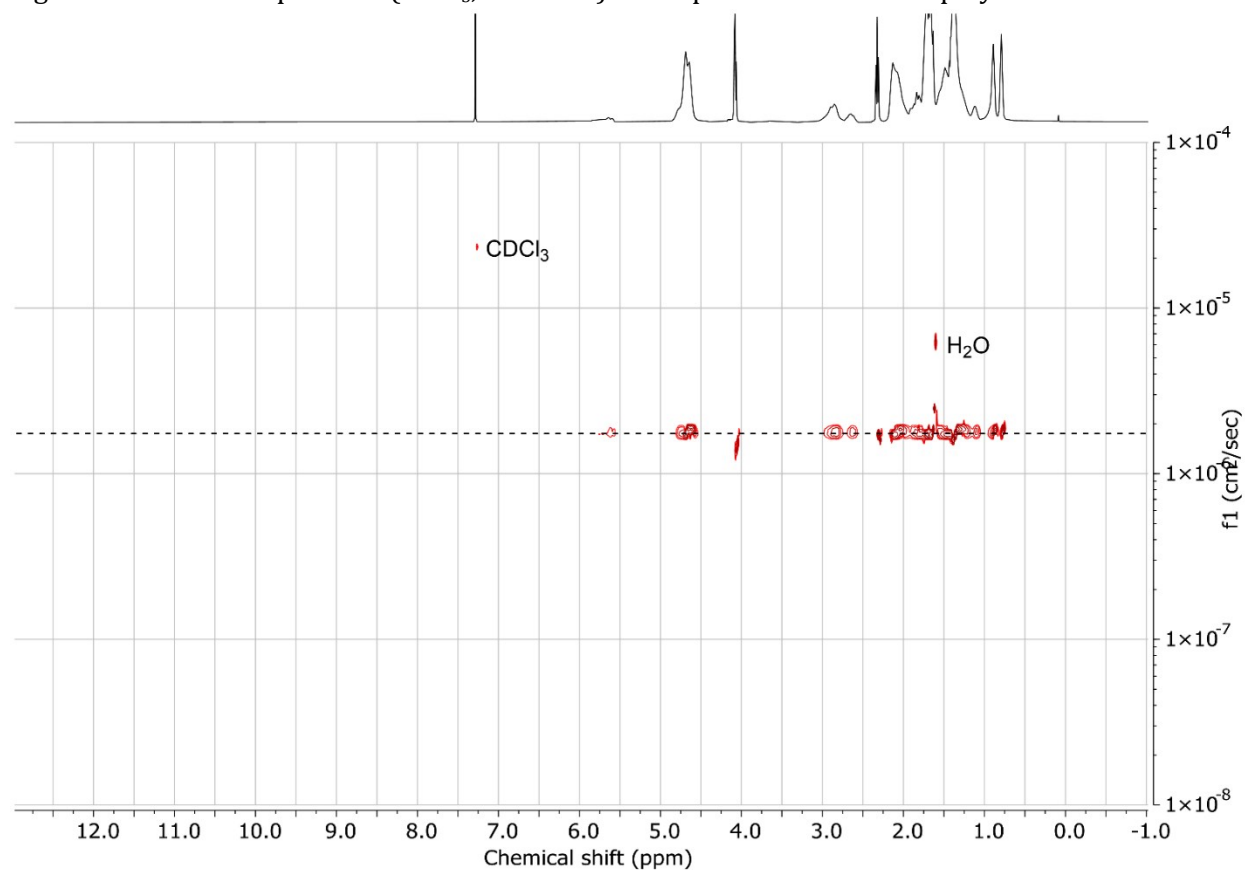


Figure S58: ¹H DOSY spectrum (CDCl₃, 500 MHz) of the purified multiblock polymer CABAC.

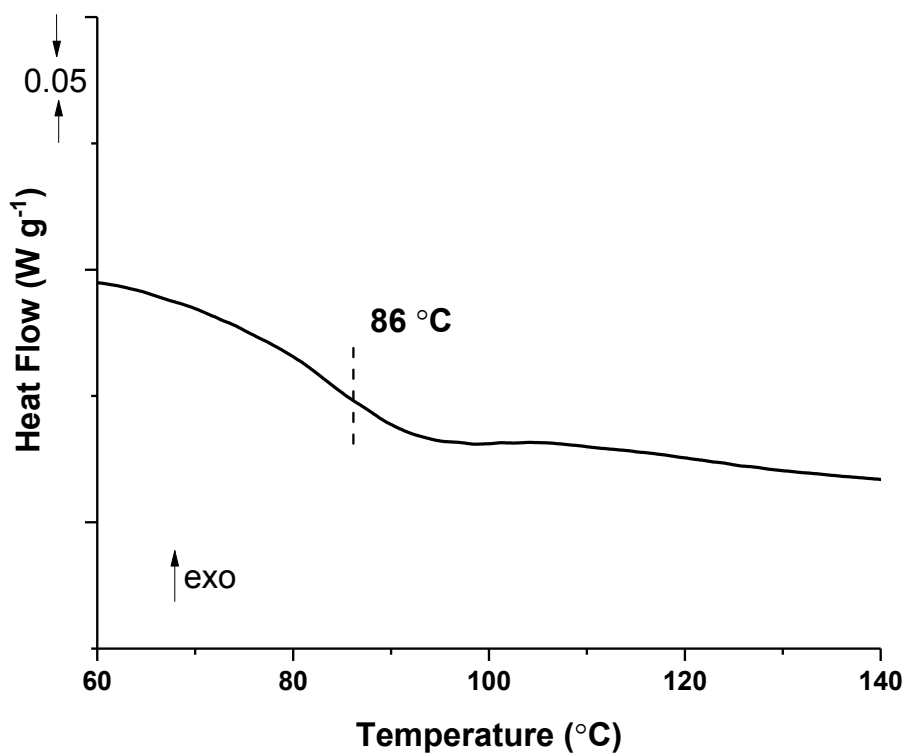


Figure S59: DSC thermogram of the purified multiblock polymer CABAC.

References

1. D. Dakshinamoorthy, A. K. Weinstock, K. Damodaran, D. F. Iwig and R. T. Mathers, *ChemSusChem*, 2014, **7**, 2923-2929.
2. A. C. Deacy, A. F. R. Kilpatrick, A. Regoutz and C. K. Williams, *Nat. Chem.*, 2020, **12**, 372-380.
3. J. A. Garden, P. K. Saini and C. K. Williams, *J. Am. Chem. Soc.*, 2015, **137**, 15078-15081.
4. M. R. Kember and C. K. Williams, *J. Am. Chem. Soc.*, 2012, **134**, 15676-15679.
5. M. R. Kember, P. D. Knight, P. T. R. Reung and C. K. Williams, *Angew. Chem. Int. Ed.*, 2009, **48**, 931-933.